

## *Faecalibacterium prausnitzii*, *Bacteroides faecis* and *Roseburia intestinalis* attenuate clinical symptoms of experimental colitis by regulating Treg/Th17 cell balance and intestinal barrier integrity

Nooshin Mohebbali<sup>a</sup>, Markus Weigel<sup>b</sup>, Torsten Hain<sup>b,c</sup>, Mona Sütel<sup>d</sup>, Jana Bull<sup>a</sup>, Bernd Kreikemeyer<sup>a,\*</sup>,<sup>1</sup>, Anne Breitrück<sup>a,1,2</sup>

<sup>a</sup> Molecular Bacteriology, Institute of Medical Microbiology, Virology and Hygiene, University Medicine Rostock, 18057 Rostock, Germany

<sup>b</sup> Institute of Medical Microbiology, Justus Liebig University, 35392 Giessen, Germany

<sup>c</sup> German Center for Infection Research (DZIF), Partner Site Giessen-Marburg-Langen, 35392 Giessen, Germany

<sup>d</sup> IMD Institut für Medizinische Diagnostik, Berlin-Potsdam GbR, 12247 Berlin, Germany

### ARTICLE INFO

#### Keywords:

IBD  
Commensal bacterial mixture  
*Faecalibacterium prausnitzii*  
*Bacteroides faecis*  
*Roseburia intestinalis*  
DSS-induced colitis

### ABSTRACT

Ulcerative colitis (UC) is a severe inflammatory bowel disease (IBD) characterized by multifactorial complex disorders triggered by environmental factors, genetic susceptibility, and also gut microbial dysbiosis. *Faecalibacterium prausnitzii*, *Bacteroides faecis*, and *Roseburia intestinalis* are underrepresented species in UC patients, leading to the hypothesis that therapeutic application of those bacteria could ameliorate clinical symptoms and disease severity. Acute colitis was induced in mice by 3.5% DSS, and the commensal bacterial species were administered by oral gavage simultaneously with DSS treatment for up to 7 days. The signs of colonic inflammation, the intestinal barrier integrity, the proportion of regulatory T cells (Tregs), and the expression of pro-inflammatory and anti-inflammatory cytokines were quantified. The concentrations of SCFAs in feces were measured using Gas-liquid chromatography. The gut microbiome was analyzed in all treatment groups at the endpoint of the experiment. Results were benchmarked against a contemporary mesalazine treatment regime. We show that commensal species alone and in combination reduced disease activity index scores, inhibited colon shortening, strengthened the colonic epithelial barrier, and positively modulated tight junction protein expression. The expression level of pro-inflammatory cytokines was significantly reduced. Immune modulation occurred via inhibition of the loss of CD4 +CD25 +Treg cells in the spleen. Our study proved that therapeutic application of *F. prausnitzii*, *B. faecis*, and *R. intestinalis* significantly ameliorated DSS-induced colitis at the level of clinical symptoms, histological inflammation, and immune status. Our data suggest that these positive effects are mediated by immune-modulatory pathways and influence on Treg/Th17 balance.

### 1. Introduction

Inflammatory bowel disease (IBD), including ulcerative colitis (UC) and Crohn's disease (CD), is a multifactorial complex disorder characterized by chronic relapsing intestinal inflammation. This disease is triggered by exogenous and endogenous factors, including genetic predisposition, environmental factors and intestinal flora. The result is chronic intestinal inflammation, epithelial barrier damage, intestinal dysbiosis, systemic inflammation, and the development of additional comorbidities [1]. Recommended treatments for IBD are corticosteroids,

immunosuppressive agents and, as novel contemporary treatment option, the amino-salicylate mesalazine. Biological agents such as monoclonal antibodies targeting proinflammatory mediators (e.g., anti-tumor necrosis factor  $\alpha$  (TNF $\alpha$ ) or anti-IL-12/IL-13 mAbs) are used as part of the treatment regimen [2]. However, the current treatment only relieves symptomatic complications and is accompanied by serious side effects, including loss of immune tolerance and drug resistance [3]. Thus there are compelling reasons to explore alternative therapeutic strategies, including prebiotics, probiotics, and symbiotics, as complementary or alternative medicines to treat IBD [4].

\* Corresponding author.

E-mail address: [bernd.kreikemeyer@med.uni-rostock.de](mailto:bernd.kreikemeyer@med.uni-rostock.de) (B. Kreikemeyer).

<sup>1</sup> Both authors contributed equally to this work.

<sup>2</sup> Current affiliation: Extracorporeal Therapy Systems (EXTHER); Fraunhofer Institute for Cell Therapy and Immunology (IZI), 18057 Rostock, Germany.

Dysbiosis of the intestinal microbiota is an endogenous factor involved in the pathogenesis of IBD [5]. A significantly decreased abundance of members of the Firmicutes phylum, particularly *Faecalibacterium prausnitzii* and *Roseburia intestinalis* was shown in clinical studies [6]. Members of this phylum produce important short-chain fatty acid metabolites such as acetate and butyrate, which provide energy for colonocytes and act as powerful anti-inflammatory substances [7,8]. Furthermore, *F. prausnitzii* and *R. intestinalis* have been shown to improve gut health in animal studies of colitis by suppressing inflammatory responses, improving gut barrier and promoting the differentiation of Treg cells [9–11]. *Bacteroides faecis*, within the *Bacteroides* genus, is a prevalent species of the human gut microbiota. Intestinal *Bacteroides* are among the most abundant and well-studied members of the mammalian commensal microbiota. They have many beneficial effects on the host, including the breakdown of complex dietary carbohydrates and the modulation of mucosal glycosylation, gene expression, angiogenesis, and immune maturation [12]. However, for most of those species the question remains how important this underrepresentation in UC development, acute and chronic disease states really is and if treatment of experimental colitis or UC patients with these species could ameliorate all clinical symptoms.

Our previous study revealed that single or mixed application of *F. prausnitzii*, *R. intestinalis* and *B. faecis* in an in vitro model of intestinal inflammation have beneficial therapeutic effects on the integrity of intestinal barrier and on inflammation processes [13]. In agreement with our findings, a number of other studies demonstrated anti-inflammatory effects both in vitro and in vivo for *F. prausnitzii* and *R. intestinalis* alone [9,10,14,15].

It is widely believed that in addition to abnormal cytokine production, imbalance of the intestinal flora [16], and barrier damage [17], UC is caused by dysregulated immune responses [18]. In particular, an abnormal T cell immune response to the intestinal flora in individuals with susceptible genes has been noted [19,20]. T-cells are a vital component of the adaptive immune system [21]. Upon activation by antigen-presenting cells, T cells differentiate into various sub-types, each equipped with a distinct set of effector functions and cytokine profiles. Four major sub-types are Th1, Th2, Th17, and regulatory T (Treg) cells. The differentiation of these T cell subsets is controlled by specific transcription factors, including T-bet, GATA3, ROR $\gamma$ t, and Foxp3 [22,23]. UC is characterized by dysregulation of the immune response involving the imbalance of Th1/Th2 and Treg/Th17 cells [24]. The excessive activation of effector T cell subsets and the concurrent deficiency of Treg cells contribute to chronic immune disorders and intestinal inflammation in UC [25]. Emerging evidence has highlighted the role of the gut microbiota and its metabolites, such as short-chain fatty acids (SCFAs), in regulation of T-cell homeostasis [26,27].

Several animal models have been developed to understand etiology and pathogenesis of IBD and to evaluate new prophylactic/therapeutic strategies [28]. For example, IL-10-deficient mice (IL-10  $-/-$ ) spontaneously develop inflammation which modifies the immune system and resembles UC in humans [29]. Chemical models, such as the DSS-induced colitis model, are the most widely used experimental models, due to simplicity, reliability, and applicability. Acute or chronic disease can be mimicked by administering adjustable concentrations of DSS in drinking water. The DSS model resembles the major clinical and histopathological features of human IBD. DSS is thought to affect intestinal epithelial cells via its toxicity. As a result, the destroyed barrier function exposes immune cells to antigens (e.g. microorganisms), triggering a subsequent immune response. Based on the characteristics of colitis, this model is suitable for studying the effect of intestinal flora on the progression of colitis. Reduced expression of tight junction proteins (e.g. occludin) in the epithelium, as well as increased intestinal permeability for luminal bacteria, are additional significant features that both human IBD and DSS-induced colitis have in common [30].

Based on our previous in vitro findings and other reports, we hypothesize that treatment with *F. prausnitzii*, *R. intestinalis* and *B. faecis*,

alone and in combination, could be a promising therapeutic strategy to modulate the pathogenesis of IBD. Consequently, in this study we use a DSS colitis mouse model to investigate if therapeutic application of 3 commensal bacterial species in diseased animals, which were found largely underrepresented in the microbiome of human UC patients, could fully ameliorate UC clinical symptoms. These experiments were benchmarked against a standard contemporary mesalazine treatment regime. Furthermore, to date, no in vivo study has investigated the effectiveness of the mixture of the 3 commensal species in a DSS colitis model. We found that *Faecalibacterium prausnitzii*, *Bacteroides faecis* and *Roseburia intestinalis*, alone and in combination prevent or ameliorate all UC associated clinical symptoms, including DAI score, colon shortening, epithelial barrier function, intestinal inflammation and immune distortion. Mechanistically, immune modulation occurred via inhibition of the loss of CD4<sup>+</sup>CD25<sup>+</sup> Treg cells in the spleen. No adverse effects of commensal bacterial treatment on the general gut microbial composition were noted. Moreover, commensal bacterial therapy performed equally well to contemporary mesalazine treatment.

## 2. Material and methods

### 2.1. The bacterial mixture

*Faecalibacterium prausnitzii* strain A2–165 (DSM 17677), *Roseburia intestinalis* (DSM 14610) and *Bacteroides faecis* (DSM 24798) were purchased from the Leibniz-Institute DSMZ GmbH (Braunschweig, Germany). All species were cultured as previously described [13]. The bacteria were grown to the mid-logarithmic phase. The inoculums were prepared to final concentrations of  $2 \times 10^9$  CFU/ml and  $2 \times 10^{10}$  CFU/ml (colony-forming units (CFU)/ml). The experiments described above were performed under strict anaerobic conditions.

### 2.2. Animals

Male C57BL/6 mice (specific pathogen-free, SPF) aged 9–11 weeks (19–25 g) were originally purchased from Charles River Laboratories (Sulzfeld, Germany). The animals were housed in a temperature-controlled environment ( $22 \pm 2$  °C) with a 12-h day/night light cycle, a relative humidity of 50–60%, and ad libitum access to rodent chow and drinking water. Individual body weights were assessed daily for eight days. All animal experiments were performed under the German animal protection law and the EU Guideline and approved by the German local authority (72221.3–1-039/19). An ARRIVE guideline [31] author checklist is provided as [supplemental material](#).

### 2.3. Experimental animal model of colitis

Experimental mice were randomly assigned into eleven groups with 11 animals per group. For group descriptions please refer to [Fig. 1](#). Acute colitis was induced by adding 3.5% (w/v) DSS (molecular weight: 35,000–50,000; MP Biomedical, LLC, Santa Ana, CA, USA) to the drinking water for 7 days. The control group received normal drinking water. *F. prausnitzii*, *B. faecis*, *R. intestinalis*, and the mixture of all three bacterial species at two concentrations of  $10^9$  CFU and  $10^{10}$  CFU per 100  $\mu$ l were administered by oral gavage simultaneously with DSS treatment for up to 7 days. Animals in the positive control group were orally administered mesalazine (200 mg/kg). Animals in the control and DSS groups were gavaged with normal PBS every day. At the end of the experimental period on day 8, the mice were anesthetized with an intraperitoneal injection of ketamine/xylazine cocktail to collect blood samples, followed by cervical dislocation. The colon, stool, and spleen were collected for further analysis.

### 2.4. Clinical evaluation of colitis

Daily assessments of weight loss, stool consistency, and fecal blood,

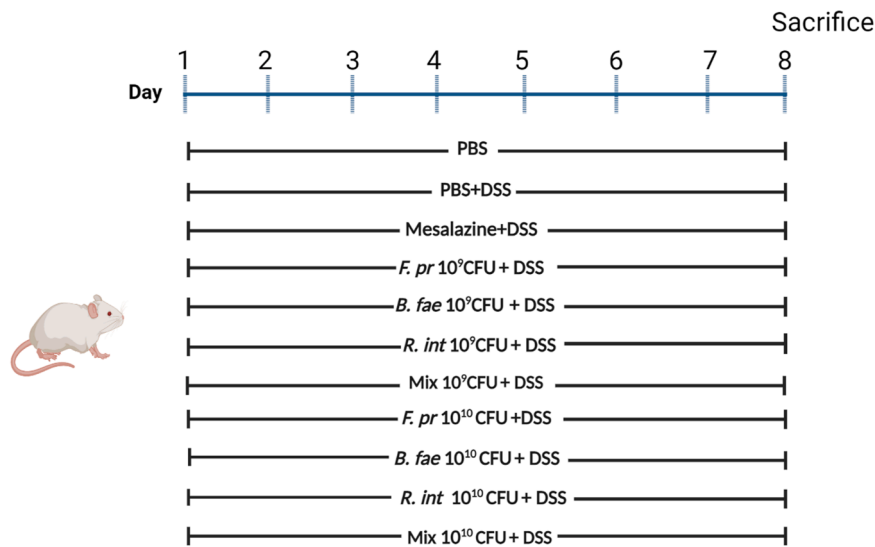


Fig. 1. Experimental design for acute colitis induction.

as indicators of the disease activity index (DAI), were performed according to the criteria described by Cooper et al. [32], with modifications (as shown in Table 1). Blood in feces was identified using a HemoCARE occult blood detection kit (Care Diagnostica, Voerde, Germany). Body weight changes were calculated relative to day 1. The sum of the weight loss, diarrhea, and bloody stool scores served as the clinical DAI.

2.5. Colon histology

After the mice were sacrificed, colon sections were collected from the mice for histological assessment. The length and weight of the colon from the anus to the appendix were measured. The colons were fixed in Roti®-Histofix 10% for 24 h before embedding in paraffin and sectioned (5 µm) with a rotary microtome. These sections were stained with hematoxylin and eosin (H&E) following the standard protocol for histopathological analysis. Histopathological changes were assessed under a light microscope by an independent observer blinded to the treatment. Histological scores were graded based on the extent of inflammation, neutrophil and lymphocyte infiltration, crypt damage, crypt abscess formation, submucosal edema, goblet cell loss, and reactive epithelial hyperplasia displayed by the sections, as shown in Table 2. The overall histopathological scores were determined by adding all the scores of the above parameters together. Colonic section were also stained with Alcian blue which targets goblet cells, using an Alcian blue/Nuclear-Fast-Red staining kit (Mophhisto). Images were obtained using a model BX53 light microscope (Olympus Optical, Tokyo, Japan).

2.6. Immunohistochemical detection of tight junction proteins

Paraffin-embedded tissue was sectioned into 5 µm slices. The sections were prepared in accordance with a published protocol [33]. The primary antibodies used for immunostaining were anti-occludin (Santa Cruz Biotechnology, #sc-133256), anti-claudin-2 (Abcam #ab53032),

Table 1  
Scoring system used to calculate the DAI.

| Score | Weight loss | Stool consistency | Visible blood in feces |
|-------|-------------|-------------------|------------------------|
| 0     | < 1%        | Normal            | None                   |
| 1     | 1%– 5%      | Slightly loose    | Slight bleeding        |
| 2     | 6%– 15%     | Loose             | Bleeding               |
| 3     | 16%– 20%    | Diarrhea          | Severe bleeding        |
| 4     | > 20%       |                   |                        |

and anti-E-cadherin (Cell Signaling #24E10), which were labeled with secondary antibodies conjugated with horseradish peroxidase (HRP) (Abcam). The sections were stained with the Liquid DAB+ 2-component system (Agilent) and counterstained with Mayer’s hematoxylin solution (Sigma—Aldrich). Histological images were acquired using a Carl Zeiss microscope.

2.7. Intestinal permeability

Intestinal epithelial permeability in vivo was determined according to a previously described method [34]. Briefly, mice were fasted for 4 h before oral gavage of a fluorescein isothiocyanate (FITC)-dextran solution (4 kDa, 600 mg/kg). Blood was harvested 3 h later by retroorbital bleeding. The blood samples were centrifuged at 1,500g for 15 min at 4 °C. Fluorescence intensity in the plasma of the mice was measured using a multimode microplate reader (SpectraMax M3, Molecular Devices) at excitation/emission wavelengths of 490/530 nm.

2.8. Myeloperoxidase (MPO) measurement

Neutrophils infiltration into the colon tissue was measured using an ELISA kit (Hycult Biotech. Inc., Plymouth Meeting, PA, USA) according to the manufacturer’s instructions.

2.9. Immunophenotyping analysis

Spleens from individual mice were collected, carefully crushed, and filtered through a 70-µm cell strainer (PluriSelect Life Science, Germany). The cells were stained with a CD4<sup>+</sup>CD25<sup>+</sup> Foxp3<sup>+</sup> regulatory T-cell staining kit (Miltenyi Biotech, Bergisch Gladbach, Germany) following the manufacturer’s instructions. Flow cytometric analysis was performed using a BD FACSVerse™ Flow Cytometer (BD Bioscience). The numbers of Tregs in the spleens were quantified and are expressed as percentages of the CD4 cell population. Postacquisition analyses were performed using FlowJo software (TreeStar, Inc., Ashland, OR).

2.10. Cytokine analysis

Colon segments were mechanically disrupted in RIPA buffer containing a phosphatase inhibitor cocktail (Santa Cruz Biotechnology, Santa Cruz, CA, USA). The homogenate was centrifuged and the supernatant was used to evaluate the levels of T helper-associated cytokines, using a multiplex cytokine magnetic bead array (BioLegend,

**Table 2**

Histological score used to quantify the degree of colitis.

| Score | Inflammation | Extent     | Regeneration                      | Crypt Damage                     | Percent Involvement |
|-------|--------------|------------|-----------------------------------|----------------------------------|---------------------|
| 0     | None         | None       | -                                 | None                             | 0%                  |
| 1     | Slight       | Mucosa     | Almost complete regeneration      | Basal 1/3 damaged                | 1%– 25%             |
| 2     | Moderate     | Mucosa+    | Regeneration with crypt depletion | Basal 2/3 damaged                | 26%– 50%            |
| 3     | Severe       | Submucosa  | Surface epithelium not intact     | Entire crypt and epithelium lost | 51%– 75%            |
| 4     |              | Transmural |                                   |                                  |                     |

Koblenz, Germany) according to the manufacturer's recommended protocol. The analysis was performed using a BD FACSVerse™ Flow Cytometer (BD Bioscience), and LEGENDplex™ Data Analysis Software was used to evaluate the data.

### 2.11. Western Blot analysis

Tight junctions protein expression in colon tissue was detected by Western Blotting. Briefly, colonic tissue was homogenized in lysis buffer. The supernatant protein concentration was measured and 25 µg of each sample was subjected SDS—PAGE according to standard methods. Then proteins were transferred to nitrocellulose membranes and blocked in 5% BSA. The membranes were incubated with primary antibodies (anti-claudin-2 #b53032, anti-occludin #ab216327, Abcam and anti-E-cadherin #3195 T Cell Signaling Technology, Inc.) at 4 °C overnight. After appropriate washing steps in PBS the membranes were subsequently incubated with IRDye®800CW goat anti-mouse and IRDye®800CW goat anti-rabbit IgG secondary antibodies. The bands were visualized and analyzed using an Odyssey imaging system (Li-Cor).

### 2.12. Microbial DNA extraction

To investigate the differential influences of the treatments on the gut microbiome, fecal samples from the last day of the experiment (day 8) were collected. The total genomic DNA was extracted from each fecal sample (approximately 50 mg) using the Quick-DNA Fecal/Soil Microbe Kit (Zymo Research) according to the manufacturer's instructions.

### 2.13. Library preparation, 16S sequencing and data analysis

The hypervariable V4 region of the included bacterial 16 S rDNA was amplified with the bacterial 16 S ribosomal RNA (rRNA)-specific primers 515 F (TCG-TCG-GCA-GCG-TCA-GAT-GTG-TAT-AAG-AGA-CAG-GTG-CCA-GCM-GCC-GCG-GTA-A) and 806 R (GTC-TCG-TGG-GCT-CGG-AGA-TGT-GTA-TAA-GAG-ACA-GGG-ACT-ACH-VGG-GTW-TCT-AAT). Amplicon PCR and index PCR, quantity and quality control, and sequencing of the individual libraries as a pool in one Illumina MiSeq run were performed as described in the Illumina "16 S Metagenomic Sequencing Library Preparation" protocol (www.illumina.com).

Sequencing using the MiSeq Reagent Kit 600v3 resulted in 58,090 to 368,468 paired-end reads per individual sample with a length of 300 nt. After quality control with Cutadapt (Version 2.8, Dortmund, Germany) [35], microbiome analysis was executed using Mothur (Version 1.46.1, Ann Arbor, MI, USA) [36], as previously described. In brief, paired-end reads were joined and filtered, and the primer sequences were removed. Reads were aligned to the SILVA ribosomal RNA gene database [37] and trimmed to the hypervariable region V4. After chimera removal, reads were clustered into a total of 17,107 OTUs representing between 24,517 and 246,209 paired-end reads. Next, the OTUs were classified against the SILVA ribosomal RNA gene database and subsampled to 24,000 reads per sample. Linear discriminant analysis effect size (LEfSe) [38] was employed to compare groups at the OTU level. Graphs were created using GraphPad Prism software version 8.0 (GraphPad Software Ltd., La Jolla, California, United States of America) and Microsoft Excel (Version

2017, Redmond, WA, USA).

In order to investigate the diversity among all experimental animal groups the homogeneity of molecular variance (HOMOVA) as a nonparametric analog of Bartlett's test for homogeneity of variance, and analysis of molecular variance (AMOVA) as a nonparametric analog of traditional analysis of variance was performed. The latter method is widely used in population genetics to test the hypothesis that genetic diversity within two populations is not significantly different from that which would result from pooling the two populations.

### 2.14. Single species detection by qPCR

Single bacterial species abundance of our treatment species was approximated using real-time quantitative PCR (qPCR). To perform the analysis, we initially extracted DNA from the corresponding stool samples using the Quick-DNA Fecal/Soil Microbe Miniprep Kit, following the manufacturer's instructions. Following DNA extraction, qPCR was carried out utilizing Maxima SYBR Green/ROX qPCR MasterMix (Thermo Scientific, Waltham, MA, United States) to characterize the gut microbiota. This characterization involved the use of species- and genus-specific primers (supplementary TableS1) targeting the 16S rRNA gene transcript. The relative gene expression was determined using the comparative delta CT-value. Negative control experiments were done without any DNA, positive controls included genomic DNA of the tested species.

### 2.15. Short chain fatty acid determination in feces

The fecal pellets were collected directly from mice at day 7 and stored at – 80 °C prior to short-chain fatty acids determination. Analysis of SCFAs was performed as previously published by Hoving et al., [39] using GC-MS/MS instrumentation (Thermo Scientific) and Chromeleon software (Thermo Scientific). The level of SCFAs is presented in µmol/g.

### 2.16. Statistical analysis

GraphPad Prism software version 8.0 (GraphPad Software Ltd., La Jolla, California, United States of America) was used to perform statistical analysis. The results are expressed as the mean ± SEM. Statistical differences between the groups were evaluated using one-way analysis of variance (ANOVA) followed by Tukey's post hoc tests. In addition, two-way ANOVA followed by Tukey's post hoc test was used to analyze DAI and body weight changes during the experimental period. Differences with  $P < 0.05$  were considered significant. Statistical significance between untreated control group versus the DSS group is marked in the figures as follows: \* $P < 0.05$ , \*\* $P < 0.01$ , \*\*\* $P < 0.001$ , \*\*\*\* $P < 0.0001$ . Statistical significance between DSS group versus the mesalazine- and bacterial species-treated groups is marked in the figures as follows # $P < 0.05$ , ## $P < 0.01$ , ### $P < 0.001$ , #### $P < 0.0001$ .

3. Results

3.1. *F. prausnitzii*, *R. intestinalis*, and *B. faecis* alleviate clinical symptoms of DSS-induced colitis in vivo

A DSS-induced acute colitis mouse model for UC was used to investigate the effects of the three commensal bacterial species individually and in combination on acute colitis development. Disease progression was assessed using classic colitis symptoms (weight loss, severe bleeding, and diarrhea). As shown in Fig. 2A, DSS treated mice exhibited progressive weight loss compared to control mice. The weight loss reached almost 10% of the initial body weight on day 8. In the groups treated with *F. prausnitzii*, *R. intestinalis*, *B. faecis* and a mixture of all three bacterial species a significant reduction in weight loss at 10<sup>9</sup> CFU (p = 0.002, p = 0.006, p = 0.636 and p = 0.040, respectively) and 10<sup>10</sup> CFU (p = 0.009, p = 0.586, p = 0.001 and p = 0.003, respectively) relative to the DSS group was noted (Fig. 2A). The results of the commensal bacteria treatment groups were comparable to those of mesalazine, which also significantly prevented weight loss following

DSS administration.

The DAI score of the DSS group increased continuously and reached a maximum at the end of the experiment (p < 0,0001). However, the DAI scores of mice treated with mesalazine, *F. prausnitzii*, *R. intestinalis*, *B. faecis*, and the mixture at both doses were significantly reduced compared to those of the DSS group (Fig. 2B-E).

In this DSS-induced mouse model, various physical symptoms appear, including changes in the length of the colon, which is a measure of intestinal inflammation. The colon length in the DSS group was significantly reduced relative to that in the control group (p < 0.001, Fig. 2F&G). Of note, DSS mice treated with bacteria (individually and in combination) exhibited significantly longer colon lengths than DSS-treated mice at 10<sup>9</sup> CFU (*F. prausnitzii*: p = 0.006; *R. intestinalis*: p = 0.056; *B. faecis*: p = 0.179; and mixture: p = 0.190) and at 10<sup>10</sup> CFU (*F. prausnitzii*: p = 0.014; *R. intestinalis*: p = 0.065; *B. faecis*: p = 0.254; and mixture: p = 0.007) (Fig. 1F, G). Mesalazine therapy of the DSS animals performed comparably to all the bacterial treatments.

Histological and morphological changes in the colon in all groups were subsequently examined by H&E staining. As shown in Fig. 2H & I,

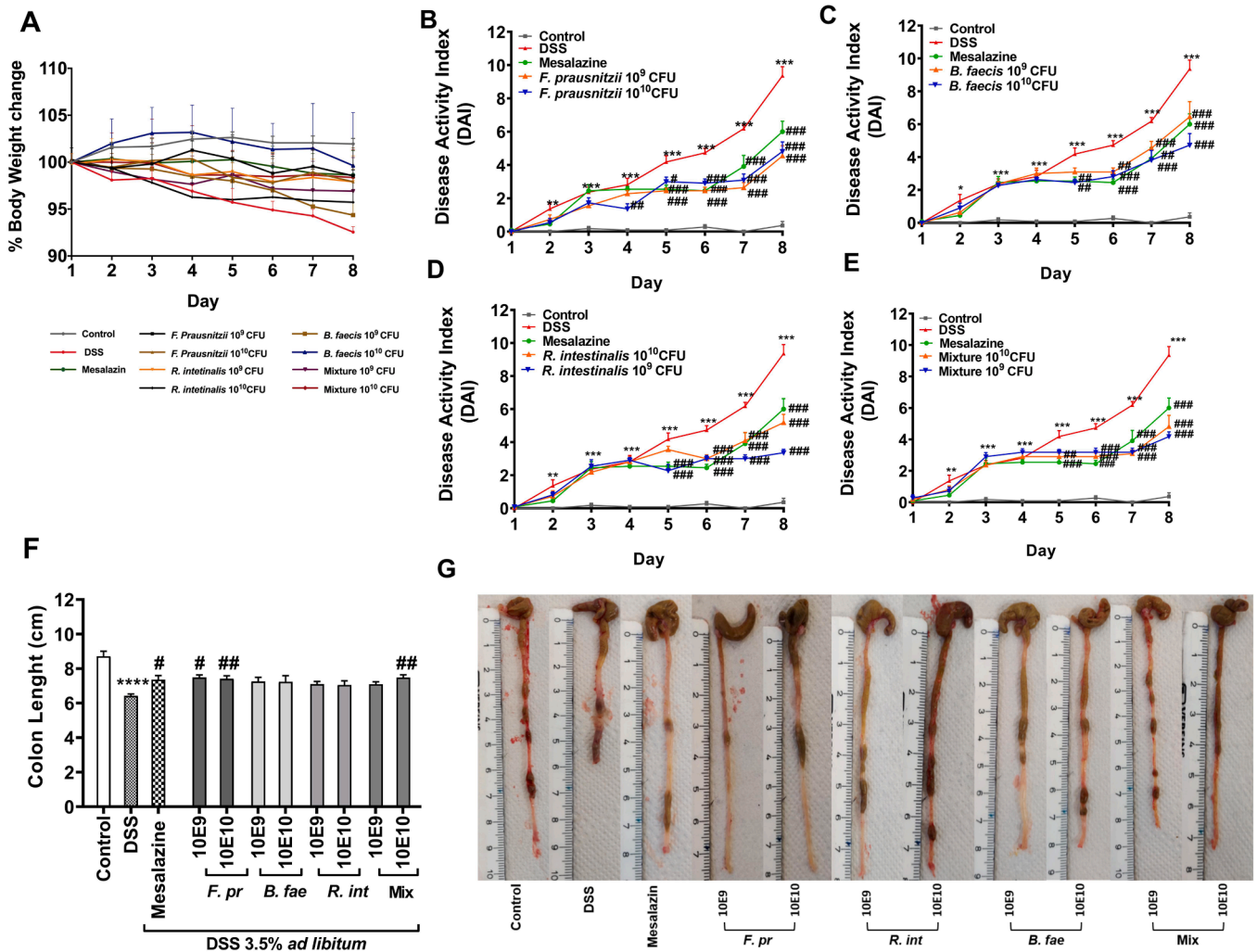


Fig. 2. Impact of *F. prausnitzii*, *B. faecis*, and *R. intestinalis* on DSS-induced colitis. (A) The body weight of mice was evaluated throughout the experiment, and the values are expressed as the percentage change from the initial value measured before DSS administration (n = 11/per group). (B-E) The disease activity index and (F) colon length were evaluated at the end of the experiment. (G) Representative pictures of colons from mice of each treatment group. (H) Colon damage was assessed by H&E staining (magnification: 10 ×). (I) Colon injury scores were allocated following histological examination. Graphs show the mean ± SEM. Statistical analysis was performed with two-way ANOVA for multiple comparison followed by the Dunnett test for comparison of the untreated control group versus the DSS group (\*\*P < 0.01, \*\*\*P < 0.001, \*\*\*\*P < 0.0001) and the mesalazine- and bacterial species-treated groups versus the DSS group (# P < 0.05, ##P < 0.01, ###P < 0.001). (J) Alcian blue staining was performed to visualize the number of goblet cells (magnification: 10 ×). The images shown are representative tissue samples from all 11 mice taken from all 11 treatment groups.

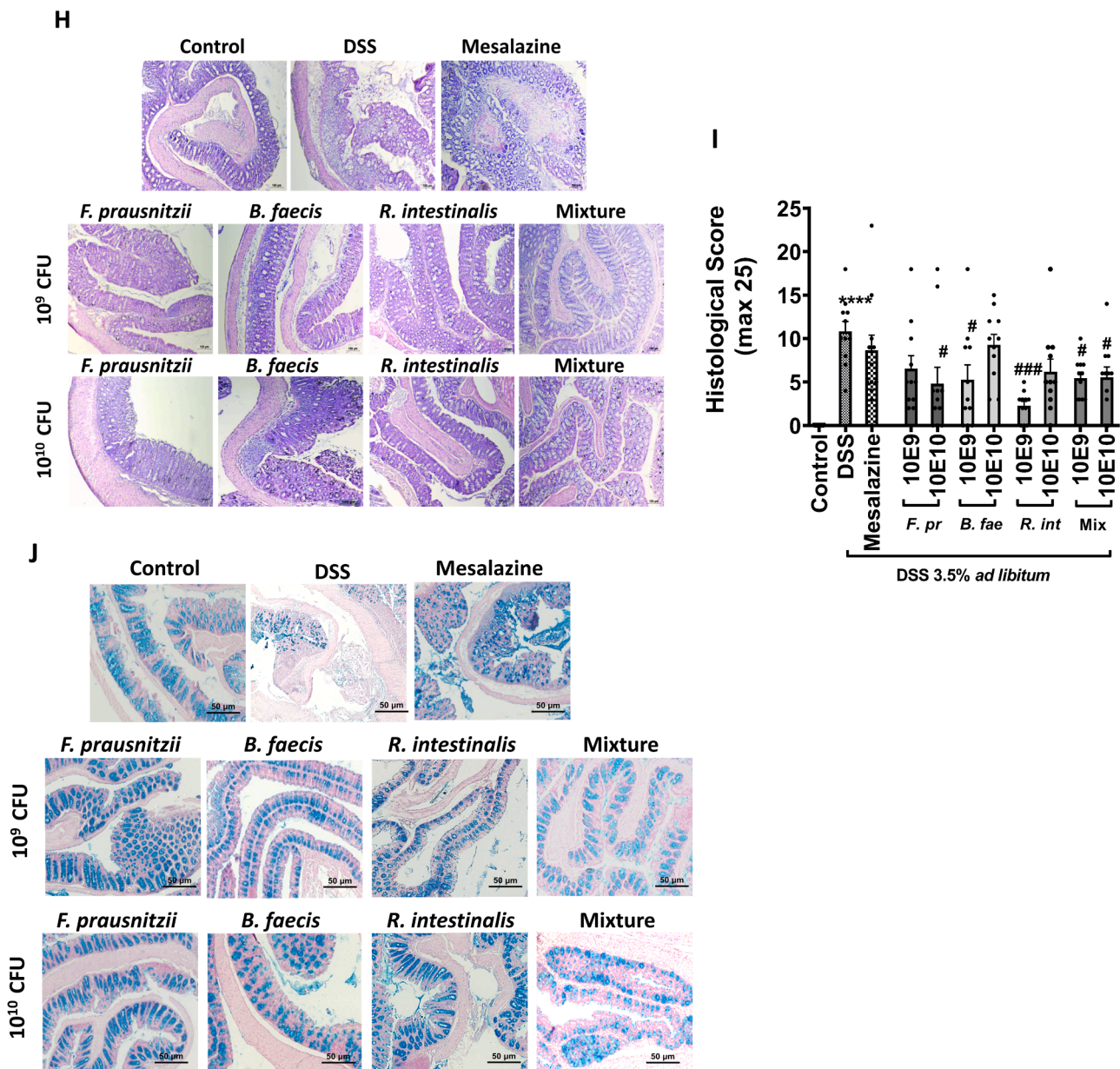


Fig. 2. (continued).

the colon structure was intact in the control group animals. The colon of DSS mice exhibited superficial ulcerations, loss of goblet cells, neutrophil infiltration, and extensive epithelial and goblet cell damage, resulting in an overall histological score of  $11.50 \pm 3.21$  ( $P < 0.0001$ ). Relative to the DSS-treated mice, the colon tissue of DSS mice treated with mesalazine, *F. prausnitzii*, *R. intestinalis*, and *B. faecis* separately and in combination at both CFUs revealed significantly less loss of goblet cells, less crypt distortion, and decreased neutrophil infiltration in the colonic mucosa. This resulted in significantly lower histological damage scores. Concerning the attenuation of severe histological damage, mesalazine was less efficient than nearly all of the bacterial treatments. Additionally, Alcian blue staining was performed to determine the number of goblet cells (Fig. 2J). The oral administration of all three bacterial species individually and in combination markedly attenuated the depletion of goblet cells.

Altogether, these results proved the efficacy of all three commensal bacterial species (both individually and in combination) in attenuating clinical symptoms in mice with DSS-induced colitis. Moreover, application of the commensal bacterial species outperformed mesalazine

therapy in alleviating and healing all evaluated types of histological damage.

### 3.2. *F. prausnitzii*, *R. intestinalis*, and *B. faecis* reduce neutrophil infiltration in colonic tissue

As another sign of intestinal inflammation we assessed neutrophil infiltration in colonic tissue by quantifying the level of myeloperoxidase (MPO). As shown in Fig. 3, MPO activity was significantly increased in the DSS group compared with the control group. The MPO concentration was visibly decreased by treatment with mesalazine and *F. prausnitzii* (at 10<sup>9</sup> CFU), however, not reaching significance level. In contrast, *F. prausnitzii* (at 10<sup>10</sup> CFU), *R. intestinalis* (at both CFU), *B. faecis* (at both CFU) and the bacterial mixture (at both CFU) lead to significantly reduced tissue MPO levels. This result revealed a positive correlation with histopathologic features and suggested that compared to mesalazine treatment, the three tested commensal bacterial species individually and in combination can equally relieve the symptoms of experimental colitis by decreasing the infiltration of neutrophils.

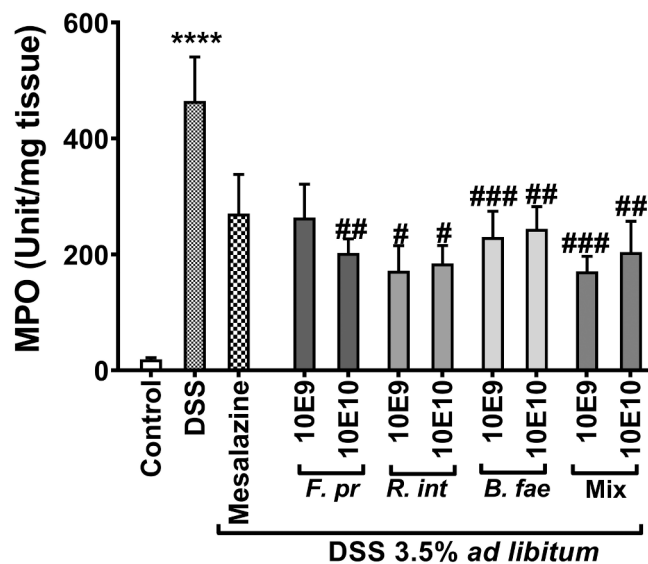


**Fig. 3.** Effect of *F. prausnitzii*, *B. faecis*, and *R. intestinalis* on myeloperoxidase (MPO) activity. The level of MPO in colonic tissue from mice with DSS-induced colitis was measured by ELISA. Data are presented as the mean  $\pm$  SEM. Statistical analysis was performed with one-way ANOVA for multiple comparison followed by the Dunnett test for comparison of the untreated control group versus the DSS group (\*\*\*\* $P < 0.0001$ ) and the mesalazine- and bacterial species-treated groups versus the DSS group (\* $P < 0.05$ , \*\* $P < 0.01$ , \*\*\* $P < 0.001$ ).

### 3.3. *F. prausnitzii*, *R. intestinalis*, and *B. faecis* improve intestinal barrier function in mice with DSS-induced colitis

Increased intestinal permeability is linked to intestinal barrier dysfunction. Therefore, we determined whether the administration of *F. prausnitzii*, *R. intestinalis*, and *B. faecis* can protect the intestinal barrier against damage induced by DSS. FITC-dextran was administered by gavage, and the intensity of fluorescence in the serum was measured 4 h later. As shown in Fig. 4A, the level of FITC-dextran in the serum of mice with DSS-induced colitis was significantly increased compared to that in the control mice. In addition, *F. prausnitzii*, *R. intestinalis*, *B. faecis* and the mixture treatment significantly reduced FITC-dextran levels in mouse plasma (for significance levels refer to Fig. 4A). Of note, all commensal bacteria performed equally well compared to the standard mesalazine therapy in our DSS mouse model.

Next, we investigated whether changes in intestinal permeability following DSS and bacterial species treatments were associated with alterations in TJ protein expression. The protein levels of occludin, E cadherin, and claudin-2 were examined by Western blotting and immunohistochemistry. As indicated in Fig. 4B-E, the expression levels of colonic E-cadherin and occludin significantly dropped in the DSS-induced colitis group compared to the control group ( $p = 0.042$  and  $p = 0.461$ , respectively). However, administration of mesalazine, *F. prausnitzii*, *B. faecis*, *R. intestinalis*, and the mixture protected mice against the loss of occludin and E-cadherin expression (for significance levels refer to Fig. 4C&D). Furthermore, claudin-2 protein expression levels were markedly increased in the DSS group compared to the control group (Fig. 4E). Following the administration of *F. prausnitzii*, *B. faecis*, and *R. intestinalis* individually and in combination, a significant decrease in claudin-2 expression was noted compared to the DSS group (Fig. 4E). Of note, some of the commensal bacterial treatments showed stronger protective effects than the mesalazine standard therapy. Supporting the TJ protein Western Blot results, immunohistochemistry experiments (Fig. 4F) also showed that the substantial decrease in occludin and E-cadherin protein levels was prevented in mice treated with the bacterial species. Moreover, compared to DSS treatment alone,

administration of all three bacterial species alleviated the altered expression of claudin-2 in the cell membrane and cytoplasm of enterocytes and glandular epithelial cells.

Altogether, these findings suggest that the three tested commensal bacterial species ameliorate the disruption of intestinal barrier function in DSS-treated mice by reducing intestinal epithelial permeability and preventing the loss of tight junction proteins.

### 3.4. Colonic tissue cytokine levels in acute DSS-induced colitis are attenuated by treatment with *F. prausnitzii*, *R. intestinalis*, and *B. faecis*

Pro-inflammatory cytokines play a crucial role in the progression of DSS-induced colitis. Consequently, we investigated the effectiveness of the three commensal bacterial species in alleviating colitis by modulation of inflammatory mediator secretion. As shown in Fig. 5A-J, the levels of Th1-type (IFN- $\gamma$ ), Th2-type (IL-13), (IL-4), and Th17-type (TNF $\alpha$ , IL-6, IL-17A, IL17F, and IL-22) cytokines were significantly enhanced exclusively in DSS-treated animals compared to the control group. The colon tissue from mice treated with all three species at both doses showed significantly reduced levels of IFN- $\gamma$ , IL-13, TNF $\alpha$ , IL-6, 17 A, 17 F, and IL-22 compared with mice in the DSS group. In contrast, secretion of the Th2-type anti-inflammatory cytokine IL-10 was slightly increased in all treatment groups, however, values did not reach significance compared with the DSS group (Fig. 5H). Moreover, the IL-10/IL-17A values of each group were investigated in order to evaluate the changes in the Th17/Treg balance. It was observed that the DSS group had significantly lower level of IL-10/IL-17A ratio compared to the control group. However, treatment with the commensal bacteria led to an increase in the IL-10/IL-17 secretion (Fig. 5J). Mesalazine was superior over all bacterial treatments only for the reduction of IL-13 levels (Fig. 5G). Altogether, these findings prove that oral administration of all three tested commensal bacteria attenuates the development of colonic inflammation in the DSS-induced colitis model via changes in Th1-type, Th2-type, and Th17-type cytokine secretion profile. The bacterial treatment regimen was comparable to mesalazine treatment in reducing cytokine levels.

### 3.5. *F. prausnitzii*, *R. intestinalis*, and *B. faecis* beneficially modulate Treg populations in DSS-induced colitis and treated mice

Dysregulation of Treg function leads to the development of inflammatory disorders, including IBD [32]. Thus, we next examined the effects of mesalazine and the selected bacterial species on Treg subset abundance in mice with DSS-induced colitis. Fig. 6A&B shows that the co-administration of all three bacterial species significantly increased the percentages of CD4 +CD25 +Foxp3 + cells at  $10^9$  CFU ( $p = 0.002$ ) and  $10^{10}$  CFU ( $p = 0.042$ ). Compared to the DSS group, the size of the CD4 +CD25 +Foxp3 +Treg population increased in the groups treated individually with *F. prausnitzii*, *B. faecis* and *R. intestinalis*, however, the increase was not statistically significant. These findings suggest that a combination of all tested commensal bacteria has a protective effect against acute DSS-induced colitis, which could partly be mediated by an increase in Treg percentages. Mesalazine therapy was comparable to the bacterial mixture in terms of Treg modulation.

### 3.6. Effect of *F. prausnitzii*, *R. intestinalis*, and *B. faecis* on SCFA contents in the feces of DSS-induced acute experimental colitis mice

Metabolites in the colon have shown associations with the symptoms of IBD [26]. The analysis of SCFAs in the collected feces showed that acetate was the most abundant acid in the feces followed by propionate and butyrate (Fig. 7A-C). The amount of SCFAs was elevated for DSS group compared to control, but these enhancements were only significant for propionate. The application of *F. prausnitzii* results in a significant lower amount of butyrate and acetate. However, no significant differences on the production of SCFAs could be detected between the

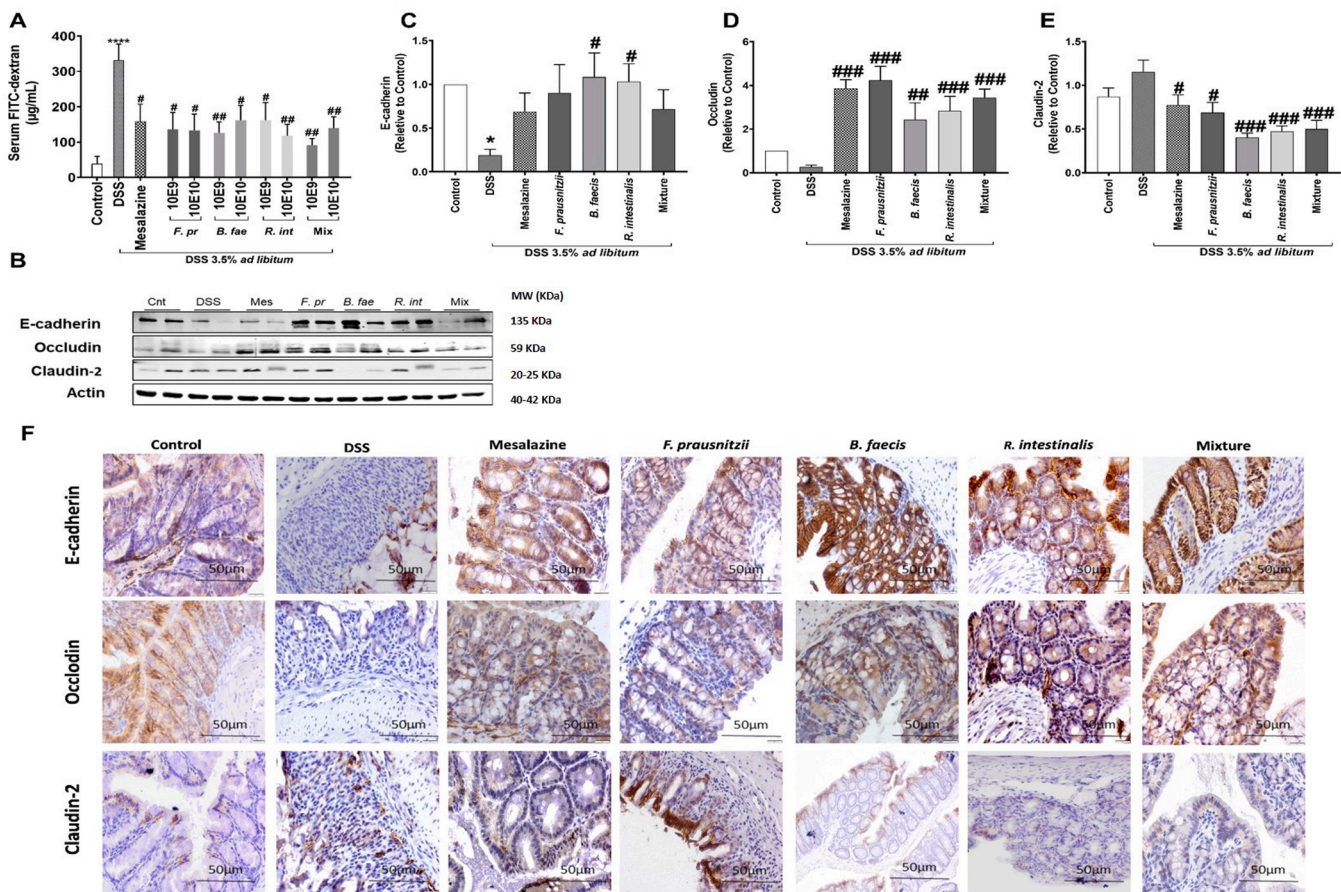


**Fig. 4.** Effect of *F. prausnitzii*, *B. faecis*, and *R. intestinalis* alone and in combination on epithelial barrier permeability and tight junction protein expression. (A) Levels of FITC-dextran in the serum of mice with DSS-induced colitis administered FITC-dextran were measured as an indicator of intestinal permeability (n = 6–10/animal per group). (B) Homogenates of colon tissue were analyzed by Western Blotting to detect the expression levels of tight junction proteins. Representative blots from 2 samples from three independent experiments are shown, and β-actin was used as a loading control. The levels of (C) E-cadherin, (D) occludin, and (E) claudin-2 expression were subsequently quantified. (F) Immunohistochemical expression patterns of the tight junction proteins in colon tissue. Magnification: 20 ×, scale bar: 50 µm. Data are presented as the mean ± SEM. Statistical analysis was performed with one-way ANOVA for multiple comparison followed by the Dunnett test for comparison of the untreated control group versus the DSS group (\*P < 0.05, \*\*\*\*P < 0.0001) and the mesalazine- and bacterial species-treated groups versus the DSS group (# P < 0.05, ### P < 0.01, #### P < 0.001).

other groups.

### 3.7. Influence of DSS and treatments on the general gut microbiome composition

From the perspective of safety and since oral treatment of DSS-treated mice with mesalazine and high doses of commensal gut microbial species could be associated with unwanted disturbance and dysbiosis of the gut microbiome, we next determined the microbiome composition of all animals at the endpoint of the experiment. A significant reduction in bacterial community richness in the DSS group compared to the control group (p < 0.0001) was observed (Fig. 8A). Mesalazine and bacterial applications did not induce significant changes in richness compared to the DSS group (Fig. 8A). Of the 16 observed phyla, Bacteroidota and Firmicutes accounted for approximately 90% of the bacteria found in the fecal microbiomes (Fig. 8B). At phylum level, the administration of *R. intestinalis* (10<sup>10</sup> CFU) and *B. faecis* (both CFU) decreased the percentages of Proteobacteria. Similar effects were observed in the gut of all mesalazine-treated animals. At genus level, we observed 231 bacterial genera. The 15 most abundant genera were typical fecal commensals with similar abundances across all treatment groups. Of note, a higher abundance of *Pelomonas* and *Methylobacterium* in all bacterial treatment groups and the mesalazine group compared to the DSS group was noted (Fig. 8C). Treatment with *F. prausnitzii*, the

bacterial mixture (10<sup>10</sup> CFU) and mesalazine slightly increased the abundance of *Lactobacillus*. Furthermore, the abundance of *Escherichia-Shigella* was decreased in all bacterial treatment groups and the mesalazine group (Fig. 8C). The microbiome data were more comprehensively evaluated by pairwise comparisons of the DSS group to each of the other groups (Supplemental Table S2). A nonparametric tool LefSe was employed. The first three OTUs (*Bacteroides*, *Prevotellaceae* unclassified, *Muribaculaceae* ge) were all in lower abundance in the control group than in the DSS group. Otu00002 was also more abundant in six of the nine treatment groups compared to the DSS group (Supplemental Table S2).

Since our chosen 16S amplicon-based microbiome analysis did not allow species-level information of the treatment bacterial species we further investigated the presence of *F. prausnitzii*, *Bacteroides* spp. and *R. intestinalis* in fecal samples using qPCR at the experimental endpoint. We used a universal primer pair for the 16 S ribosomal RNA coding sequence as endogenous control. The average expression of selected bacterial genes was calculated by comparative delta CT. qPCR results showed that exclusively *Bacteroides* spp. was detectable and present in all animals, with significant changes comparing the mixture group versus DSS group. (Fig. 8D, Supplemental TableS3). The sample CT-values for *F. prausnitzii* and *R. intestinalis* were in most cases below the detection limit (data not shown).

To show the basic characteristics of the gut microbiota profile

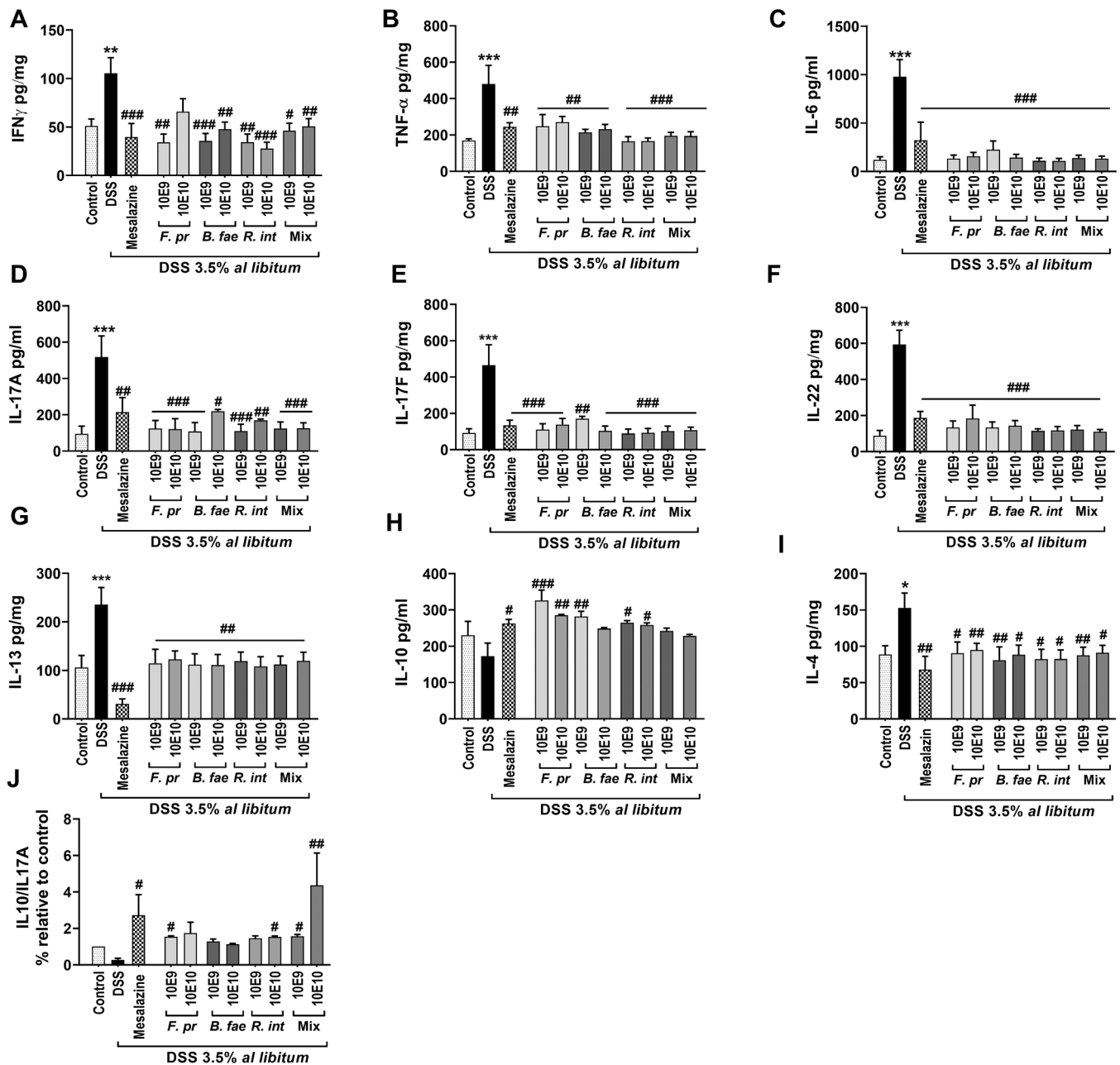


**Fig. 5.** Regulation of the innate immune response in the colon by *F. prausnitzii*, *B. faecis*, and *R. intestinalis*. The expression levels of the cytokines IFN- $\gamma$ , TNF $\alpha$ , IL-6, IL-17 F, IL17A, IL-22 IL-13,IL-4 and IL-10 in colon tissue were detected by multiplex ELISA. Data are shown as the means  $\pm$  SEMs (n = 11). Statistical analysis was performed with one-way ANOVA followed by the Dunnet test for comparison of the untreated control group versus the DSS group (\*\*P < 0.01, \*\*\*P < 0.001) and the mesalazine- and bacterial species-treated groups versus the DSS group (# P < 0.05, ##P < 0.01, ###P < 0.001).

between the groups we performed  $\beta$ -diversity analysis. The DSS treatment changed the  $\beta$ -diversity significantly, whereas no changes in  $\beta$ -diversity upon any of our treatments could be detected (see supplemental Fig. 1). Basically, all DSS-treated groups are closer to each other compared to the untreated control, who form a distinct cluster (determined by Homogeneity of molecular variance (HOMOVA) and Analysis of molecular variance (AMOVA)).

Cumulatively, these results suggest that the microbiome was nearly unaltered by our treatments and that the bacterial species used for treatment were most likely present only transiently.

#### 4. Discussion

The cause of IBD is multifactorial, but it is well recognized that

disturbed intestinal bacterial homeostasis may contribute to the onset and progression of IBD. In addition, several studies have indicated that the diversity and composition of the gastrointestinal tract microbiota in IBD patients are altered (Fig. 9) [4–6]. Although an increasing number of bacterial species are associated with IBD and have been tested in animal models and clinical trials, the exact molecular mechanism of the protective effect of these bacteria is still unclear.

Our previous results proved the barrier-strengthening and anti-inflammatory potential of *F. prausnitzii*, *R. intestinalis*, and *B. faecis* commensals in vitro [13]. Consequently, the present in vivo study evaluated the therapeutic potential of the three commensals in an experimental DSS-induced colitis model in comparison with a standard mesalazine therapy regimen.

In our study, we observed that individual and combined

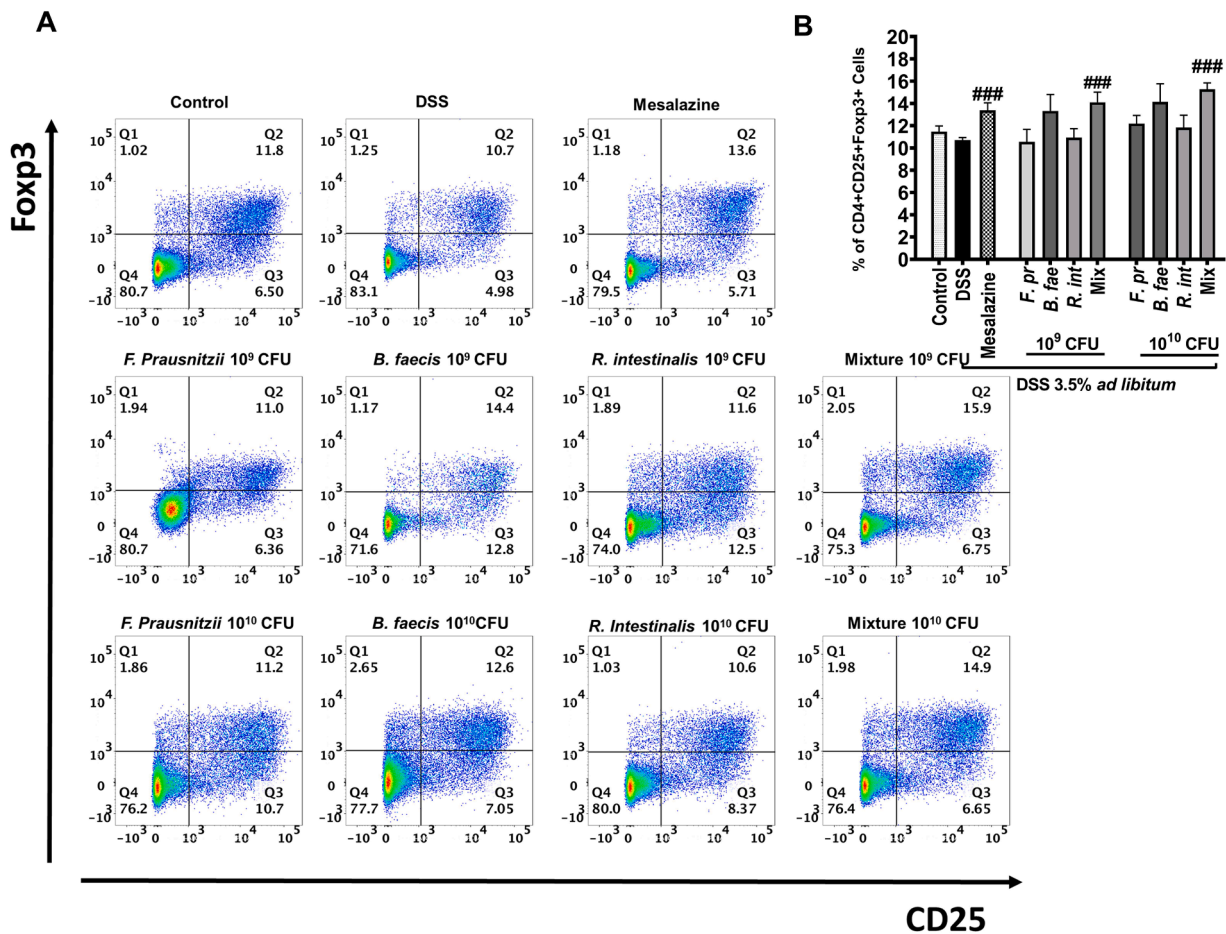


**Fig. 6.** *F. prausnitzii*, *B. faecis*, and *R. intestinalis* alone and in combination expand the Treg population in mice with experimental colitis. The mice were sacrificed, and their spleens were isolated. To detect Tregs, the spleens were stained with anti-mouse CD4, CD25, and Foxp3 mAbs as described in the Materials and Methods. (A). Treg percentages were analyzed by FACS. (B) Data are shown as the means  $\pm$  SEMs (n = 11). Statistical analysis was performed by the Mann–Whitney U test versus the DSS+PBS group. (###P < 0.001).

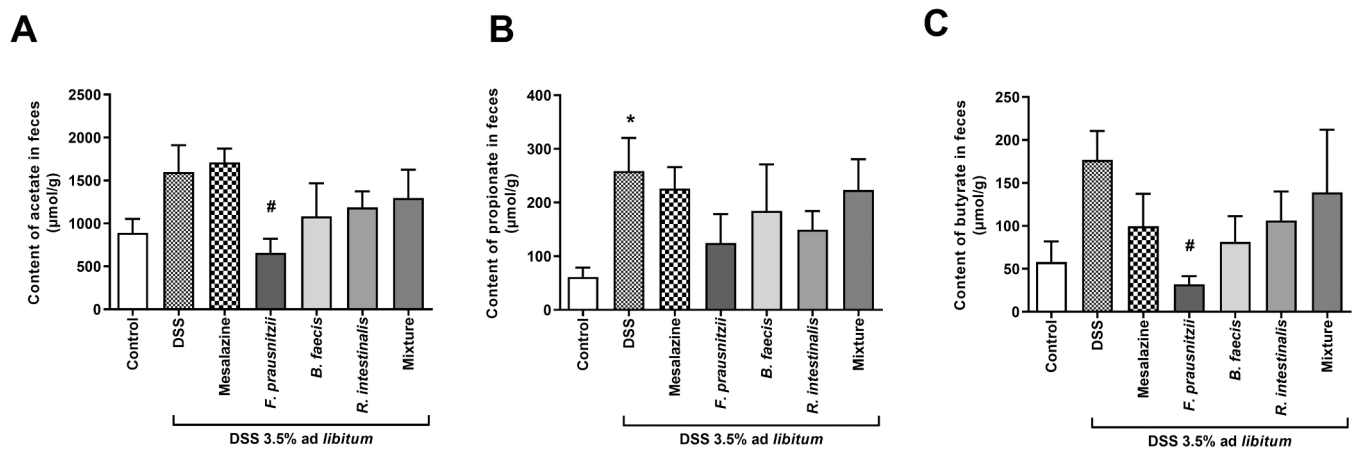


**Fig. 7.** Alterations in the fecal short chain fatty acids content due to DSS and bacterial treatment. Data are shown as the means  $\pm$  SEMs (n = 5 (control, DSS, mesalazine, *F. prausnitzii*, *R. intestinalis*); n = 4 (mixture); n = 3 (*B. faecis*)). Statistical analysis was performed with one-way ANOVA followed by the Dunnet test for comparison of the untreated control group versus the DSS group (\*P < 0.05) and the mesalazine- and bacterial species-treated groups versus the DSS group (# P < 0.05).

administration of *F. prausnitzii*, *B. faecis*, and *R. intestinalis* effectively attenuated the severity of DSS-induced colitis in mice (Fig. 9). Furthermore, reduced DAI scores and inhibited colon shortening at both doses was found. Additionally, the decrease in MPO activity in the colon

of DSS-treated mice after oral administration of the commensals suggests their ability to reduce the infiltration of granulocytes and hence, the inflammatory reactions (Fig. 9). Probiotics and potential probiotic commensal bacteria have been shown to have a variety of mechanisms

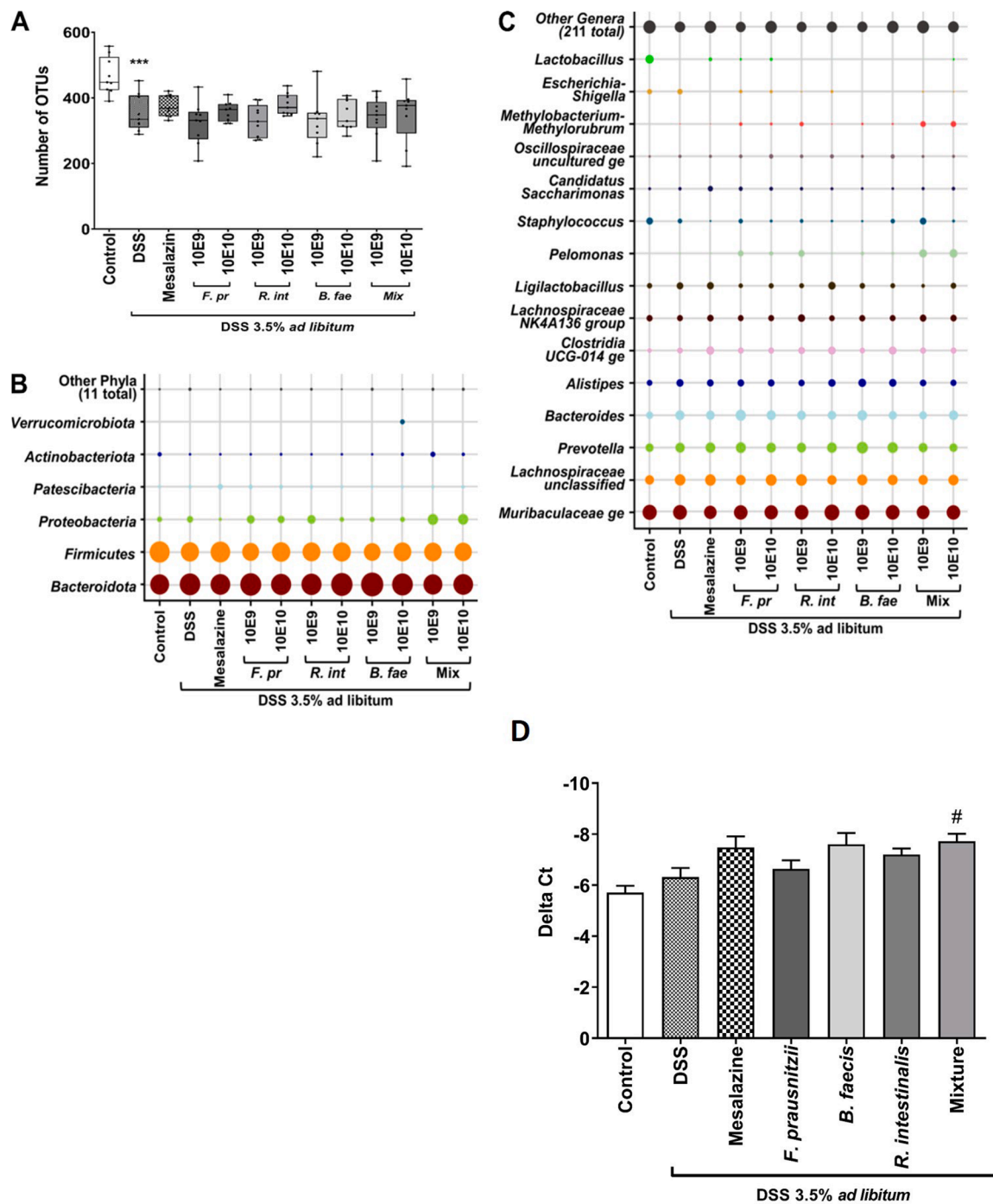


**Fig. 8.** Alterations in the fecal microbiome due to DSS and bacterial treatments. (A) Number of distinct operational taxonomic units (OTUs) observed in the different treatment groups. (B) Phyla found in the fecal microbiome with a relative abundance of at least 0.5%. (C) Top 15 genera found in the eleven treatment groups by overall relative abundance. (D) q-PCR detection of *Bacteroides* spp. showing the relative abundance with universal bacterial primers listed in [supplementary Tables1](#). Data are shown as the means ± SEMs (n = 7 (control, DSS, mesalazine, *F. prausnitzii*); n = 6 (*R. intestinalis*, *B. faecis*, mixture)). Statistical analysis was performed with one-way ANOVA followed by Dunnett’s test for comparison of the untreated control group versus the DSS group (\*\*P < 0.01).

of action. These include enhancing epithelial barrier function, preventing pathogenic bacteria from colonizing the epithelium, producing antimicrobial compounds, and modulating the immune system [40].

Inflammatory bowel disease is associated with a disturbed intestinal epithelial barrier caused by pathologically altered tight junction proteins. One potential mechanism leading to the observed changes in barrier function is cytokine secretion from lymphocytes infiltrating the lamina propria (Fig. 9). Numerous studies have shown that inflammatory responses influence TJ protein expression. For instance, a higher

concentration of pro-inflammatory cytokines (such as IFN- $\gamma$ , TNF- $\alpha$ , and IL-1 $\beta$ ) reduces the expression of tight junction proteins, thereby increasing epithelial paracellular permeability [41,42]. Moreover, Th2 cytokines such as IL-4 and IL-13 have also been shown to affect tight junction proteins in the intestinal epithelium by upregulating the expression of Claudin-2 [43,44]. In addition, IL-13 can downregulate the expression of occludin and ZO-1, leading to increase paracellular permeability [44].

In our study, oral administration of all three tested commensal

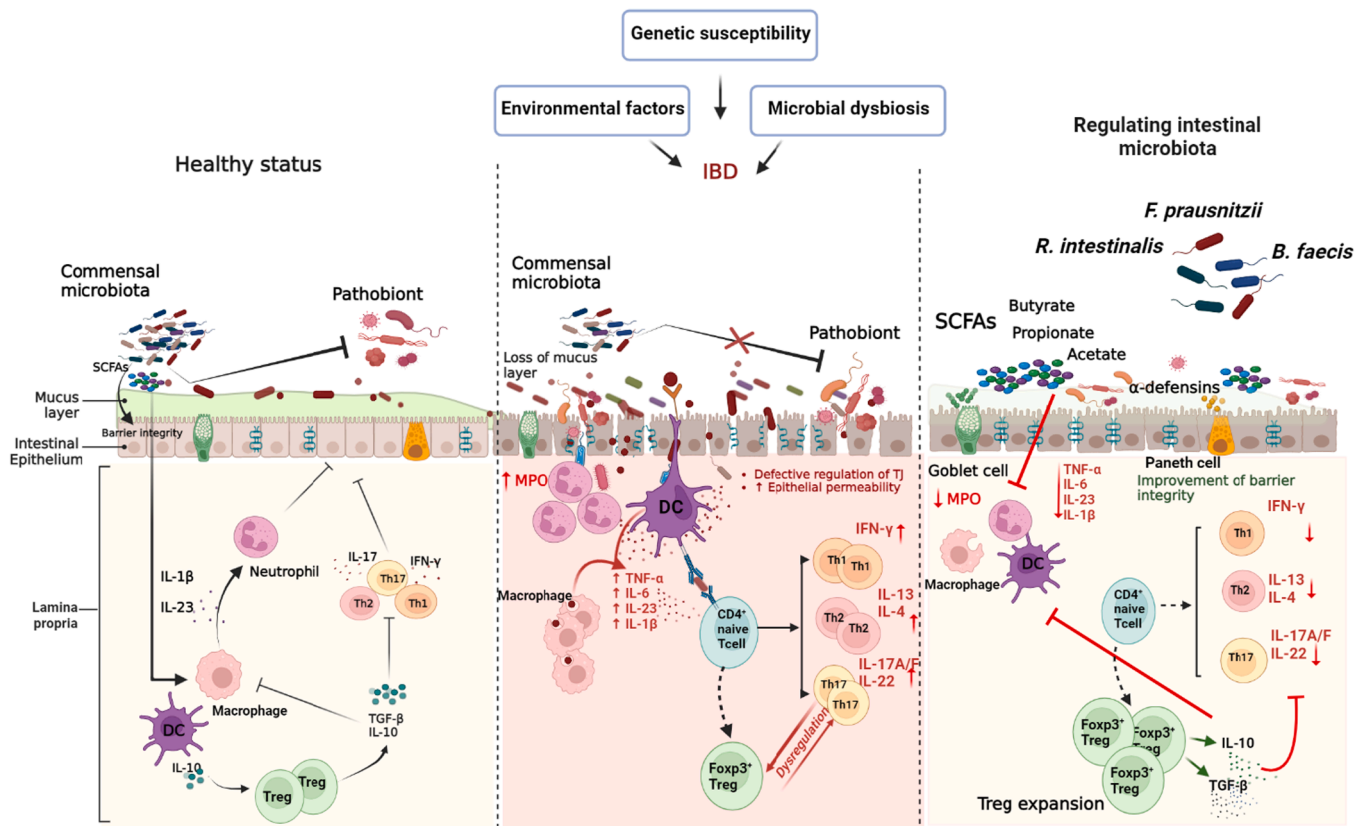


Fig. 9. Schematic illustration of the underlying protective mechanisms of *F. prausnitzii*, *B. faecis*, and *R. intestinalis* against DSS-induced experimental colitis via restoration of the Treg/Th17 balance.

bacteria, individually and in combination, significantly affected the expression levels of tight junction proteins, indicating restoration of the epithelial barrier (Fig. 9). This positive outcome was confirmed by the barrier function improvement, as seen in the in vivo FITC-dextran permeability assay. We also observed that secretion levels of IFN-γ, TNFα, IL-6, IL-17, IL-22, IL-4, and IL-13 in the colon tissue were significantly elevated by DSS treatment and were markedly suppressed by the administration of the tested commensal bacteria at both doses. Several studies have demonstrated similar effects of probiotics such as *Lactobacillus GG*, *Bifidobacterium breve*, *B. bifidum*, and *R. gnavus* on intestinal barrier function [45,46].

Even though the exact pathogenesis of IBD is not yet clear, evidence suggests that Th17 and Treg cells have a functional antagonism, in which Tregs act as immunosuppressive cells, and Th17 cells are involved in initiating autoimmune and inflammatory diseases [47]. Treg cells, characterized by Foxp3 expression, are essential regulators of immunological homeostasis and tolerance by regulating the release of the inhibitory cytokines IL-10, IL-4, and IL-13 [48]. Conversely, Th17 cells are involved in the development of various autoimmune diseases and producing pro-inflammatory cytokines such as IL-17A [49]. Research has shown that patients with inflammatory bowel disease have reduced levels of CD4 + CD25 + Treg cells in their peripheral blood and elevated levels of IL-17A compared to healthy individuals [50,51].

Notably, the diversity of gut microbiota and its metabolites have a significant impact on modulating the Treg/Th17 balance, which in turn affects the inflammatory responses associated with IBD; the microbiota can induce Th17 cells, leading to aggravated colitis in mouse models while SCFAs, which are microbiota-derived metabolites, promote the differentiation of Treg cells [52]. Consistent with this observation, our results showed that the Treg and T17 cell balance is disturbed in DSS-administered mice, and the number of CD4 + CD25 + Foxp3 + Treg cells in the spleen of mice with untreated colitis was lower than that in

the control group. Moreover, there was a notable increase in the secretion of IL-17A and IL-17 F cytokines due to the infiltration of Th17 cells to the site of inflammation in the intestine, resulting in the activation of the mucosal immune system and increased secretion of pro-inflammatory cytokines. However, in DSS-induced colitis mice, oral administration of *F. prausnitzii*, *B. faecis*, and *R. intestinalis* increased the percentage of CD4 + CD25 + Foxp3 + cells in the spleen, with more pronounced Treg induction when the mixture of the tested species was administered. Of note, the secretion of IL-17 A and IL-17-F was significantly decreased in the bacterial-treated groups.

Shen et al. conducted an in vivo study which revealed that *R. intestinalis* can impede the progression of inflammation in mice with TNBS-induced colitis by promoting Treg differentiation [53]. Furthermore, an increase in the expression level of the potent immunoregulatory cytokine IL-10 was observed in mice with DSS-induced colitis treated with all three bacterial species and their mixture. Remarkably, the IL-10/IL-17A ratio was significantly higher in the DSS-treated group than in the control and bacterial-treated groups, supporting the hypothesis that Th17 cells induce IL-17A secretion during inflammation. However, the IL-10 secretion was induced by *F. prausnitzii*, *B. faecis*, and *R. intestinalis* intervention, which effectively reversed the IL-10/IL-17A ratio.

This finding indicated that commensal bacterial species alone and in combination had protective effects against the development of DSS-induced colitis, which were at least partly mediated by regulating Treg/Th17 cell balance. Huang et al. also found similar results in their studies, demonstrating that the *Lactobacillus paracasei* R3 strain can improve the overall symptoms of colitis by inhibiting Th17 function and promoting Treg function in DSS-induced colitis mice [54]. Similarly, Martin et al. showed that *F. prausnitzii* induces Foxp3 + and Treg production in the spleen during TNBS-induced colitis [11]. These findings suggested that enhancing the activity of suitable Tregs in the gut might

aid in the restoration of inflamed colonic tissues, making Tregs a prospective target for treating UC.

SCFAs are a product of the gut microbiota and changes within the composition of the microbiota due to intestinal inflammation are accompanied by altered SCFA levels [55]. Clinical studies in UC patients have reported reduced levels of SCFAs [15,56,57]. However, the investigation of SCFAs in DSS colitis models is contradictory, with both reduced and increased concentrations reported [58–61]. The determination of SCFAs in feces samples from day 7 in our study showed the highest values in the DSS colitis group, which was significant for proportionate. This result was unexpected but a potential explanation is the fact that SCFAs are taken up by the colonic epithelial cells. This could explain why only low levels can be measured in the feces [62,63]. It is also possible that the diseased tissue in the DSS group at the experimental endpoint is attenuated in its capacity to take up and efficiently metabolized the produced SCFAs leading to accumulation of these substances. This points to a limitation of our study and in follow up experiments also earlier time points should be considered for SCFAs quantification. Furthermore, SCFA concentrations in feces depend also on transit time, as clinical studies with irritable bowel syndrome patients with predominant diarrhea (IBS-D) and in vivo IBS mice models have shown increased level of SCFAs [64–66]. An increased transit time inhibits the uptake of SCFAs by the colonic epithelial cells, leading to higher SCFAs concentrations in the feces. Diarrhea is a hallmark clinical sign in induced DSS colitis, which is represented within the DAI score. Therefore, an increased DAI score in DSS mice and decreased DAI score for bacterial treatment groups could be associated with our results.

The diversity and composition of the gut microbiota are crucial for the progression of IBD. Accumulating evidence suggests that alterations in the gut microbial composition lead to metabolite changes affecting the pathogenesis of IBD [67,68]. Therefore, the gut microbiome was studied in all treatment groups at the endpoint of the experiment. At the phylum level, the *R. intestinalis* and *B. faecis* treatments decreased the abundance of Proteobacteria to a lower level than that in the control group. Most Proteobacteria are LPS-producing, harmful gram-negative bacteria [69], with *Escherichia-Shigella* as a typical genus. Although Proteobacteria were found in a higher abundance in the bacterial treatment groups, at the genus and OTU levels, *Escherichia-Shigella* were less abundant in all treatment groups. The depletion of *Lactobacillus* has been shown in UC patients [70], and DSS colitis [71,72], which is consistent with our results from the DSS group. However, bacterial treatment with *F. prausnitzii* and the mixture did not restore the abundance of this genus or *Lactobacillus* OTUs to normal levels. We observed several changes in the gut microbiota composition related to the genera *Muribaculaceae* and *Lachnospiraceae*. Most of the significant differences between groups explained by LEfSe were for OTUs with a relative abundance of less than 1%, which indicates that the microbiome of the probiotic treatment groups was not impacted in a significant way compared to that of the DSS group. The importance of the increase in OTU00002 in most treatment groups is hard to estimate because of the limiting classification at the family level. Further comparison against the NCBI nucleotide collection with Blast did not provide further insight into the genus or species associated with this OTU. The absence of *F. prausnitzii*, *R. intestinalis*, and *B. faecis* could demonstrate the transient nature of the probiotic treatment or could therefore be a side effect of the endpoint measurement, which is a clear limitation of our study. Nevertheless, this outcome could indicate the safety of this commensal bacterial treatment approach, as the treatment does not permanently influence the fecal microbiome, which is very important for potential future clinical use of our bacterial cocktail.

Treatment studies with the focus on balancing microbial gut dysbalances occurring in IBD are still an emerging field [21,22]. Of note, recently, *Akkermansia muciniphila* was proven to successfully counteract deleterious dysbalances induced by dietary emulsifiers [73]. To our knowledge, the current study is the first to investigate the influence of the commensal bacterial species *F. prausnitzii*, *R. intestinalis*, and *B. faecis*

as single or mixed formulations on the DSS-induced colitis mouse model.

There are, however, some limitations to our study. Although the animal model we used closely resembles some histopathological and immunological characteristics of patients with IBD, it does not fully represent all of the complex features of the disease. Therefore, additional longitudinal studies should be carried out using various mouse strains and animal models. Furthermore, the exact mechanisms underlying the anti-inflammatory and immunoregulatory effects of the tested species should be identified in future research. Additionally, more research is needed to gain insight into the potential microbiome-modulating properties of the bacterial treatments by analyzing the abundance of gut microbes at different time points during the experimental protocol. In particular qPCR experiments and detection of SCFAs should be performed more dynamically at all time points of the animal experiments and from various animal materials (tissue, blood, stool) and not just as endpoint measurements. We also envision an additional study using our bacterial treatment cocktail in a model studying protection against multiple episodes of DSS-induced dysbalances. This would address the aspect of chronic relapsing episodes of UC in patients.

In summary, we demonstrated that application of commensal bacteria alone or in mixture alleviated the severity of DSS-induced colitis in a mice model and reduced body weight loss, the DAI, colon length and histological inflammation. The underlying mechanisms of the therapeutic commensals intervention effect are schematically depicted in Fig. 9 and included restoring intestinal barrier integrity by increased expression of tight junction proteins, regulation of inflammatory response and intestinal microbiota modulation. Our data suggest that these positive effects are likely mediated by immune-modulatory pathways and influence on Treg/Th17 balance. Notably, the commensal therapy was found to be equally effective as the contemporary mesalazine treatment. Taken together, these findings prove the potential of the commensal mixture as an effective therapeutic strategy for IBD. Future studies with this bacterial cocktail in humans are therefore well justified and required as a next step to evaluate the value and the safety of this therapeutic approach.

#### Data deposition

Microbiome sequencing data have been submitted to the NCBI Short Read Archive repository under the BioProject accession number PRJNA906496 (<https://www.ncbi.nlm.nih.gov/sra/PRJNA906496>).

#### Patient and public involvement statement

Patients were not involved at this stage of our research study.

#### Institutional review board statement

All animal experiments were performed in compliance with the German animal protection law, and were approved by the local animal care and use committee (Project ID: 7221.3-1-039/19, Approval date: October 08, 2019).

#### Funding

This study was supported by the German Research Foundation (DFG KFO 309 Z01, SFB1021 Z02, SFB-TR84 B08) and HMWK LOEWE Research Cluster Diffusible Signals project B3 to T.H. This research was funded by a DAMP Foundation-grant (number 2017-01) awarded to B.K.

#### CRediT authorship contribution statement

**Nooshin Mohebali:** Conceptualization, Formal analysis, Investigation, Writing – original draft, Writing – review & editing, Visualization. **Markus Weigel:** Formal analysis, Data curation. **Torsten Hain:** Formal analysis, Data curation, Funding acquisition. **Mona Sütel:** Investigation.

**Jana Bull:** Investigation. **Bernd Kreikemeyer:** Conceptualization, Investigation, Writing – original draft, Writing – review & editing, Supervision, Project administration, Funding acquisition. **Anne Breitrück:** Conceptualization, Formal analysis, Investigation, Writing – original draft, Writing – review & editing, Supervision, Project administration.

### Declaration of Competing Interest

The authors declare that they have no known competing financial interests or personal relationships that could have appeared to influence the work reported in this paper.

### Data Availability

The data that support the findings of this study are available from the authors on reasonable request, see author contributions for specific data sets. Microbiome sequencing data have been submitted to the NCBI Short Read Archive repository under the BioProject accession number PRJNA694316 (<https://www.ncbi.nlm.nih.gov/sra/PRJNA694316>).

### Appendix A. Supporting information

Supplementary data associated with this article can be found in the online version at [doi:10.1016/j.biopha.2023.115568](https://doi.org/10.1016/j.biopha.2023.115568).

### References

- I. Loddo, C. Romano, *Inflammatory bowel disease: genetics, epigenetics, and pathogenesis*, *Front. Immunol.* vol. 6 (2015) 551.
- K. Hazel, A. O'Connor, Emerging treatments for inflammatory bowel disease, *Ther. Adv. Chronic Dis.* vol. 11 (2020), 2040622319899297, <https://doi.org/10.1177/2040622319899297>.
- J.K. Triantafyllidis, E. Merikas, F. Georgopoulos, Current and emerging drugs for the treatment of inflammatory bowel disease: (2011). Current and emerging drugs for the treatment of inflammatory bowel disease, in: *Drug design, development and therapy*, 5, Drug Design, Development and Therapy, 2011, p. 185, <https://doi.org/10.2147/DDDT.S11290>.
- Israr Khan, et al., Alteration of gut microbiota in inflammatory bowel disease (IBD): cause or consequence? IBD treatment targeting the gut microbiome, *Pathogens* vol. 8 (3) (2019) 126, <https://doi.org/10.3390/pathogens8030126>.
- J. Li, et al., Gut microbiota dysbiosis contributes to the development of hypertension, *Microbiome* vol. 5 (1) (2017), 14, <https://doi.org/10.1186/s40168-016-0222-x>.
- E.A. Ahmed, S.M. Ahmed, N.H. Zakaria, N.M. Baddour, D.A. Header, Study of the gut microbiome in Egyptian patients with active ulcerative colitis, *Rev. De Gastroenterol. De Mex* (2022), <https://doi.org/10.1016/j.rgmex.2022.07.006>.
- W. Peng, H. Ao, C. Peng, Gut microbiota, short-chain fatty acids, and herbal medicines, *Front. Pharmacol.* vol. 9 (2018), 1354, <https://doi.org/10.3389/fphar.2018.01354>.
- H. Sokol, et al., Faecalibacterium prausnitzii is an anti-inflammatory commensal bacterium identified by gut microbiota analysis of Crohn disease patients, *Proc. Natl. Acad. Sci. USA* vol. 105 (43) (2008) 16731–16736, <https://doi.org/10.1073/pnas.0804812105>.
- C. Zhu, et al., Roseburia intestinalis inhibits interleukin-17 excretion and promotes regulatory T cells differentiation in colitis, *Mol. Med. Rep.* vol. 17 (2018) 7567–7574, <https://doi.org/10.3892/mmr.2018.8833>.
- W. Luo, et al., Roseburia intestinalis supernatant ameliorates colitis induced in mice by regulating the immune response, *Mol. Med. Rep.* vol. 20 (2019) 1007–1016, <https://doi.org/10.3892/mmr.2019.10327>.
- R. Martín, et al., The commensal bacterium Faecalibacterium prausnitzii is protective in DNBS-induced chronic moderate and severe colitis models, *Inflamm. Bowel Dis.* vol. 20 (2014) 417–430, <https://doi.org/10.1097/01.MIB.0000440815.76627.64>.
- L.V. Hooper, M.H. Wong, A. Thelin, L. Hansson, P.G. Falk, J.I. Gordon, Molecular analysis of commensal host-microbial relationships in the intestine, *Science* vol. 291 (5505) (2001) 881–884, <https://doi.org/10.1126/science.291.5505.881>.
- N. Mohebali, K. Ekbat, B. Kreikemeyer, A. Breitrück, Barrier protection and recovery effects of gut commensal bacteria on differentiated intestinal epithelial cells in vitro, *Nutrients* vol. 12 (2020), <https://doi.org/10.3390/nu12082251>.
- E. Quévrain, et al., Identification of an anti-inflammatory protein from Faecalibacterium prausnitzii, a commensal bacterium deficient in Crohn's disease, *Gut* vol. 65 (3) (2016) 415–425, <https://doi.org/10.1136/gutjnl-2014-307649>.
- K. Machiels, et al., A decrease of the butyrate-producing species Roseburia hominis and Faecalibacterium prausnitzii defines dysbiosis in patients with ulcerative colitis, *Gut* vol. 63 (2014) 1275–1283, <https://doi.org/10.1136/gutjnl-2013-304833>.
- H. Takaishi, et al., Imbalance in intestinal microflora constitution could be involved in the pathogenesis of inflammatory bowel disease, *Int. J. Med. Microbiol.* IJMM vol. 298 (5–6) (2008) 463–472, <https://doi.org/10.1016/j.ijmm.2007.07.016>.
- H. Schmitz, et al., Epithelial barrier and transport function of the colon in ulcerative colitis, *Ann. N. Y. Acad. Sci.* vol. 915 (1) (2000) 312–326.
- X.-R. Xu, C.-Q. Liu, B.-S. Feng, Z.-J. Liu, Dysregulation of mucosal immune response in pathogenesis of inflammatory bowel disease, *World J. Gastroenterol.* vol. 20 (2014) 3255–3264, <https://doi.org/10.3748/wjg.v20.i12.3255>.
- R.B. Sartor, Mechanisms of Disease: pathogenesis of Crohn's disease and ulcerative colitis, *Nat. Clin. Pract. Gastroenterol. Hepatol.* vol. 3 (2006) 390–407, <https://doi.org/10.1038/ncpgasthep0528>.
- W. Strober, I.J. Fuss, Proinflammatory cytokines in the pathogenesis of inflammatory bowel diseases, *Gastroenterology* vol. 140 (2011) 1756–1767, <https://doi.org/10.1053/j.gastro.2011.02.016>.
- Y.-Z. Zhang, Y.-Y. Li, *Inflammatory bowel disease: pathogenesis*, *World J. Gastroenterol.* WJG vol. 20 (1) (2014) 91.
- Susanne J. Szabo, Sean T. Kim, Gina L. Costa, Xiankui Zhang, C. Garrison Fathman, Laurie H. Glimcher, A novel transcription factor, T-bet, directs Th1 lineage commitment, no. 6, *Cell* vol. 100 (2000) 655–669, [https://doi.org/10.1016/S0092-8674\(00\)80702-3](https://doi.org/10.1016/S0092-8674(00)80702-3).
- Ivaylo I. Ivanov, et al., The orphan nuclear receptor ROR $\gamma$ t directs the differentiation program of proinflammatory IL-17+ T helper cells, *Cell* vol. 126 (6) (2006) 1121–1133, <https://doi.org/10.1016/j.cell.2006.07.035>.
- J. Yao, C. Wei, J.-Y. Wang, R. Zhang, Y.-X. Li, L.-S. Wang, Effect of resveratrol on Treg/Th17 signaling and ulcerative colitis treatment in mice, no. 21, *World J. Gastroenterol.* vol. 21 (2015) 6572–6581, <https://doi.org/10.3748/wjg.v21.i21.6572>.
- A. Izcue, J.L. Coombes, F. Powrie, Regulatory lymphocytes and intestinal inflammation, *Annu. Rev. Immunol.* vol. 27 (2009) 313–338, <https://doi.org/10.1146/annurev.immunol.021908.132657>.
- A. Lavelle, H. Sokol, Gut microbiota-derived metabolites as key actors in inflammatory bowel disease, *Nat. Rev. Gastroenterol. Hepatol.* vol. 17 (4) (2020) 223–237, <https://doi.org/10.1038/s41575-019-0258-z>.
- N. Arpaia, et al., Metabolites produced by commensal bacteria promote peripheral regulatory T-cell generation, *Nature* vol. 504 (7480) (2013) 451–455, <https://doi.org/10.1038/nature12726>.
- J.A. Jimenez, T.C. Uwiera, G. Douglas Inglis, R.R.E. Uwiera, Animal models to study acute and chronic intestinal inflammation in mammals, *Gut Pathog.* vol. 7 (2015), 29, <https://doi.org/10.1186/s13099-015-0076-y>.
- N. Hoshi, et al., MyD88 signalling in colonic mononuclear phagocytes drives colitis in IL-10-deficient mice, *Nat. Commun.* vol. 3 (1) (2012), 1120, <https://doi.org/10.1038/ncomms2113>.
- T. Hudcovic, R. Stěpánková, J. Cebra, H. Tlaskalová-Hogenová, The role of microflora in the development of intestinal inflammation: acute and chronic colitis induced by dextran sulfate in germ-free and conventionally reared immunocompetent and immunodeficient mice, *Folia Microbiol.* vol. 46 (2001) 565–572, <https://doi.org/10.1007/BF02818004>.
- N. Du Percie Sert, et al., The ARRIVE guidelines 2.0: updated guidelines for reporting animal research, *PLoS Biol.* vol. 18 (2020), e3000410, <https://doi.org/10.1371/journal.pbio.3000410>.
- H.S. Cooper, S.N. Murthy, R.S. Shah, D.J. Sedergran, *Clinicopathologic study of dextran sulfate sodium experimental murine colitis*, *Lab. Invest.* ; a J. Tech. *Methods Pathol.* vol. 69 (2) (1993) 238–249.
- T.E. Riehl, S. Santhanam, L. Foster, M. Ciorba, W.F. Stenson, CD44 and TLR4 mediate hyaluronic acid regulation of Lgr5+ stem cell proliferation, crypt fission, and intestinal growth in postnatal and adult mice, *Am. J. Physiol. Gastrointest. Liver Physiol.* vol. 309 (11) (2015) G874–87, <https://doi.org/10.1152/ajpgi.00123.2015>.
- V. Volynets, A. Reichold, G. Bárdos, A. Rings, A. Bleich, S.C. Bischoff, Assessment of the intestinal barrier with five different permeability tests in healthy C57BL/6J and BALB/cJ mice, *Dig. Dis. Sci.* vol. 61 (3) (2016) 737–746, <https://doi.org/10.1007/s10620-015-3935-y>.
- M. Martin, Cutadapt removes adapter sequences from high-throughput sequencing reads, *EMBnet J.* vol. 17 (1) (2011) 10, <https://doi.org/10.14806/ej.17.1.200>.
- J.J. Kozich, S.L. Westcott, N.T. Baxter, S.K. Highlander, P.D. Schloss, Development of a dual-index sequencing strategy and curation pipeline for analyzing amplicon sequence data on the MiSeq Illumina sequencing platform, *Appl. Environ. Microbiol.* vol. 79 (17) (2013) 5112–5120, <https://doi.org/10.1128/AEM.01043-13>.
- C. Quast, et al., The SILVA ribosomal RNA gene database project: improved data processing and web-based tools, *Nucleic Acids Res.* vol. 41 (Database issue) (2013) D590–6, <https://doi.org/10.1093/nar/gks1219>.
- N. Segata, et al., Metagenomic biomarker discovery and explanation, *Genome Biol.* vol. 12 (6) (2011) R60, <https://doi.org/10.1186/gb-2011-12-6-r60>.
- L.R. Hoving, M. Heijink, V. van Harmelen, K.W. van Dijk, M. Giera, GC-MS analysis of short-chain fatty acids in feces, cecum content, and blood samples, *Clin. Metab.: Methods Protoc.* (2018) 247–256.
- L. Prisciandaro, M. Geier, R. Butler, A. Cummins, G. Howarth, Probiotics and their derivatives as treatments for inflammatory bowel disease, *Inflamm. Bowel Dis.* vol. 15 (12) (2009) 1906–1914, <https://doi.org/10.1002/ibd.20938>.
- L.W. Kaminsky, R. Al-Sadi, T.Y. Ma, IL-1 $\beta$  and the intestinal epithelial tight junction barrier, *Front. Immunol.* vol. 12 (2021), 767456, <https://doi.org/10.3389/fimmu.2021.767456>.
- T.Y. Ma, et al., TNF-alpha-induced increase in intestinal epithelial tight junction permeability requires NF-kappa B activation, *Am. J. Physiol. Gastrointest. Liver Physiol.* vol. 286 (3) (2004) G367–76, <https://doi.org/10.1152/ajpgi.00173.2003>.

- [43] S. Prasad, et al., "Inflammatory processes have differential effects on claudins 2, 3 and 4 in colonic epithelial cells," *Lab. Investig. ; a J. Tech. Methods Pathol.* vol. 85 (9) (2005) 1139–1162.
- [44] F. Heller, et al., Interleukin-13 Is the key effector Th2 cytokine in ulcerative colitis that affects epithelial tight junctions, apoptosis, and cell restitution, *Gastroenterology* vol. 129 (2) (2005) 550–564, <https://doi.org/10.1053/j.gastro.2005.05.002>.
- [45] L. Zhang, N. Li, R. Caicedo, J. Neu, Alive and dead *Lactobacillus rhamnosus* GG decrease tumor necrosis factor- $\alpha$ -induced interleukin-8 production in Caco-2 cells, *J. Nutr.* vol. 135 (7) (2005) 1752–1756, <https://doi.org/10.1093/jn/135.7.1752>.
- [46] R.K. Rao, G. Samak, Protection and restitution of gut barrier by probiotics: nutritional and clinical implications, *Curr. Nutr. Food Sci.* vol. 9 (2) (2013) 99–107, <https://doi.org/10.2174/1573401311309020004>.
- [47] M. Noack, P. Miossec, Th17 and regulatory T cell balance in autoimmune and inflammatory diseases, *Autoimmun. Rev.* vol. 13 (6) (2014) 668–677, <https://doi.org/10.1016/j.autrev.2013.12.004>.
- [48] L. Fan, et al., B. adolescentis ameliorates chronic colitis by regulating Treg/Th2 response and gut microbiota remodeling, *Gut Microbes* vol. 13 (1) (2021) 1–17, <https://doi.org/10.1080/19490976.2020.1826746>.
- [49] G.J. Britton, et al., Microbiotas from humans with inflammatory bowel disease alter the balance of Gut Th17 and ROR $\gamma$ t+ regulatory T cells and exacerbate colitis in mice, *Immunity* vol. 50 (1) (2019) 212–224.e4, <https://doi.org/10.1016/j.immuni.2018.12.015>.
- [50] X. Geng, J. Xue, Expression of Treg/Th17 cells as well as related cytokines in patients with inflammatory bowel disease, *Pak. J. Med. Sci.* vol. 32 (5) (2016) 1164.
- [51] M.J. McGeachy, D.J. Cua, S.L. Gaffen, The IL-17 family of cytokines in health and disease, *Immunity* vol. 50 (4) (2019) 892–906, <https://doi.org/10.1016/j.immuni.2019.03.021>.
- [52] P.M. Smith, et al., The microbial metabolites, short-chain fatty acids, regulate colonic Treg cell homeostasis, *Science* vol. 341 (6145) (2013) 569–573, <https://doi.org/10.1126/science.1241165>.
- [53] Z. Shen, et al., Roseburia intestinalis stimulates TLR5-dependent intestinal immunity against Crohn's disease, *EBioMedicine* vol. 85 (2022), 104285, <https://doi.org/10.1016/j.ebiom.2022.104285>.
- [54] J. Huang, et al., *Lactobacillus paracasei* R3 protects against dextran sulfate sodium (DSS)-induced colitis in mice via regulating Th17/Treg cell balance, *J. Transl. Med.* vol. 19 (1) (2021), 356, <https://doi.org/10.1186/s12967-021-02943-x>.
- [55] M. Rajilić-Stojanović, et al., Intestinal microbiota and diet in IBS: causes, consequences, or epiphenomena? *Am. J. Gastroenterol.* vol. 110 (2) (2015) 278–287, <https://doi.org/10.1038/ajg.2014.427>.
- [56] W. Yang, Y. Cong, Gut microbiota-derived metabolites in the regulation of host immune responses and immune-related inflammatory diseases," *Cell. Mol. Immunol.* vol. 18 (4) (2021) 866–877.
- [57] M. Sun, W. Wu, Z. Liu, Y. Cong, Microbiota metabolite short chain fatty acids, GPCR, and inflammatory bowel diseases, *J. Gastroenterol.* vol. 52 (2017) 1–8.
- [58] S. Singh, et al., Anti-inflammatory Bifidobacterium strains prevent dextran sodium sulfate induced colitis and associated gut microbial dysbiosis in mice, *Sci. Rep.* vol. 10 (1) (2020), 18597, <https://doi.org/10.1038/s41598-020-75702-5>.
- [59] L.A. Maslin, B.R. Weeks, R.J. Carroll, D.H. Byrne, N.D. Turner, Chlorogenic acid and quercetin in a diet with fermentable fiber influence multiple processes involved in dss-induced ulcerative colitis but do not reduce injury, *Nutrients* vol. 14 (18) (2022), <https://doi.org/10.3390/nu14183706>.
- [60] T. Ishida, et al., Oyster (*Crassostrea gigas*) extract attenuates dextran sulfate sodium-induced acute experimental colitis by improving gut microbiota and short-chain fatty acids compositions in mice, *Foods* vol. 11 (3) (2022), <https://doi.org/10.3390/foods11030373>.
- [61] Q. Zou, et al., Ficus carica polysaccharide attenuates DSS-induced ulcerative colitis in C57BL/6 mice, *Food Funct.* vol. 11 (7) (2020) 6666–6679, <https://doi.org/10.1039/D0FO01162B>.
- [62] D.L. Topping, P.M. Clifton, Short-chain fatty acids and human colonic function: roles of resistant starch and nonstarch polysaccharides, *Physiol. Rev.* vol. 81 (3) (2001) 1031–1064, <https://doi.org/10.1152/physrev.2001.81.3.1031>.
- [63] G. den Besten, K. van Eunen, A.K. Groen, K. Venema, D.-J. Reijngoud, B.M. Bakker, The role of short-chain fatty acids in the interplay between diet, gut microbiota, and host energy metabolism, *J. Lipid Res.* vol. 54 (9) (2013) 2325–2340, <https://doi.org/10.1194/jlr.R036012>.
- [64] G. Gargari, et al., Fecal Clostridiales distribution and short-chain fatty acids reflect bowel habits in irritable bowel syndrome, *Environ. Microbiol.* vol. 20 (9) (2018) 3201–3213, <https://doi.org/10.1111/1462-2920.14271>.
- [65] Q. Sun, Q. Jia, L. Song, L. Duan, Alterations in fecal short-chain fatty acids in patients with irritable bowel syndrome: a systematic review and meta-analysis, *Medicine* vol. 98 (7) (2019) [Online]. Available: [https://journals.lww.com/md-journal/fulltext/2019/02150/alterations\\_in\\_fecal\\_short\\_chain\\_fatty\\_acids\\_in.64.aspx](https://journals.lww.com/md-journal/fulltext/2019/02150/alterations_in_fecal_short_chain_fatty_acids_in.64.aspx).
- [66] I.F. Shaidulloev, D.M. Sorokina, F.G. Sitdikov, A. Hermann, S.R. Abdulkhakov, G. F. Sitdikova, Short chain fatty acids and colon motility in a mouse model of irritable bowel syndrome, *BMC Gastroenterol.* vol. 21 (1) (2021), 37, <https://doi.org/10.1186/s12876-021-01613-y>.
- [67] J.-S. Park, et al., *Lactobacillus acidophilus* improves intestinal inflammation in an acute colitis mouse model by regulation of Th17 and Treg cell balance and fibrosis development, *J. Med. Food* vol. 21 (3) (2018) 215–224.
- [68] Woon-Ki Kim, You Jin Jang, Boram Seo, Dae Hee Han, SungJun Park, GwangPyo Ko, Administration of *Lactobacillus paracasei* strains improves immunomodulation and changes the composition of gut microbiota leading to improvement of colitis in mice, *J. Funct. Foods* vol. 52 (2019) 565–575, <https://doi.org/10.1016/j.jff.2018.11.035>.
- [69] T. Ohkusa, S. Koido, Intestinal microbiota and ulcerative colitis, *J. Infect. Chemother.: Off. J. Jpn. Soc. Chemother.* vol. 21 (11) (2015) 761–768, <https://doi.org/10.1016/j.jiac.2015.07.010>.
- [70] P. Yu, C. Ke, J. Guo, X. Zhang, B. Li, *Lactobacillus plantarum* L15 alleviates colitis by inhibiting LPS-Mediated NF- $\kappa$ B activation and ameliorates DSS-induced gut microbiota dysbiosis, *Front. Immunol.* vol. 11 (2020), 575173, <https://doi.org/10.3389/fimmu.2020.575173>.
- [71] Niu, M.M., Guo, H.X., Cai, J.W., & Meng, X.C., Bifidobacterium breve Alleviates DSS-Induced Colitis in Mice by Maintaining the Mucosal and Epithelial Barriers and Modulating Gut Microbes: (2022). Bifidobacterium breve Alleviates DSS-Induced Colitis in Mice by Maintaining the Mucosal and Epithelial Barriers and Modulating Gut Microbes. *Nutrients*, 14(18), 3671., *Nutrients*, vol. 14, no. 18, 2022, doi: 10.3390/nu14183671.
- [72] S.J. Ott, Reduction in diversity of the colonic mucosa associated bacterial microflora in patients with active inflammatory bowel disease, *Gut* vol. 53 (5) (2004) 685–693, <https://doi.org/10.1136/gut.2003.025403>.
- [73] N. Daniel, A.T. Gewirtz, B. Chassaing, Akkermansia muciniphila counteracts the deleterious effects of dietary emulsifiers on microbiota and host metabolism, *Gut* (2023), <https://doi.org/10.1136/gutjnl-2021-326835>.